Quantifying AAV (hM3Dq) transfection in neocortical cells as a guide to DREADDs control of trauma-induced epileptogenesis

Mémoire

Ali Reza Danesh

Maîtrise en neurosciences - avec mémoire
Maître ès sciences (M. Sc.)

Québec, Canada

Quantifying AAV (hM3Dq) transfection in neocortical cells

as a guide to DREADDs control of trauma-induced epileptogenesis

Mémoire

Ali Reza Danesh

Sous la direction de :

Dr Igor Timofeev

Résumé

Le néocortex déclenche des activités paroxystiques suite aux lésions cérébrales traumatiques. Avec des blessures cérébrales pénétrantes, la déafférentation s'accompagne d'une longue période silencieuse du cortex atteint, et d'une augmentation des périodes d'hyperpolarisation du néocortex entourant la lésion. L'activité synchrone du réseau neuronal après une période de latence conduirait à l'épileptogenèse. Des tentatives de modifier la nature des crises ont été effectuées à l'aide de modèles animaux. L'une des plus prometteuse étant la chimiogenèse par l'injection des vecteurs viraux afin d'anéantir la réponse de certains récepteurs couplés aux protéines G aux ligands habituels, alors qu'ils réagissent aux médicaments désirés, comme N-oxyde de clozapine. Ces récepteurs appelés « DREADDs » exclusivement activés par ces médicaments ont été étudiés pour réduire le nombre et la sévérité des crises. Selon les résultats non-publiés de notre laboratoire, l'utilisation d'un DREADD excitateur près de «undercut» serait antiépileptogène. Nous pensons qu'une excitation ciblée pourrait optimiser l'effet antiépileptogène. L'excitation est directement liée aux neurones transduits. Nous postulons qu'une transduction optimale des neurones pourrait être atteinte par un dosage optimisé du virus injecté, tant au titre viral qu'au volume injecté. Pour prouver notre hypothèse nous avons utilisé trois différentes titrations de AAV2/8 et injecté différents volumes de ces titrations aux souris. Le volume de transfection corticale et le nombre des neurones transduits ont été quantifiés. Avec la titration E11gc/ml aucune transfection n'a été observée. Avec la titration E12gc/ml une corrélation quasi-linéaire a été observée entre le volume viral injecté, et le volume cortical transfecté, ainsi que le nombre de neurones transduits. Avec la titration E13gc/ml, une meilleure corrélation a été observée à la transduction neuronale qu'à la transfection corticale, par rapport au volume viral injecté. En conclusion, la titration E12gc/ml paraît être un meilleur choix pour nos futures études, la fiabilité de la titration E13gc/ml n'ayant pas été démontrée.

Abstract

The neocortex is the origin of paroxysmal activities that occur after traumatic brain injuries. In penetrating brain injuries, deafferentation causes long silent periods in affected cortex and increased hyperpolarization period in neocortical tissue around the injury. The synchronous neural network activity after a latent period may lead to epileptogenesis. Some attempts to alter seizures were done using animal models. One of the most promising involves chemogenetic tools via AAV viral vector injection to make some G protein-coupled receptors unresponsive to their natural ligands, and activated by the desired drug, such as clozapine-N-oxide. These designer receptors exclusively activated by designer drugs (DREADDs) have been studied in reducing the numbers and severity of seizures. According to unpublished works in our lab, using excitatory DREADDs in the vicinity of undercut was antiepileptogenic. We believe there could be an optimal level of excitation for yielding an optimal antiepileptogenic response. This excitation is in direct relation with neurons transfected. We hypothesize that the optimal neuronal transduction might be achieved with optimal dosage of virus delivered, in terms of viral titration and the volume of virus injected. To test this, we used three different titrations of AAV2/8 and we injected different volumes of these titrations in adult mice. Cortical transfection volume and number of neuronal transductions were estimated. With E11gc/ml titration, no transfection was visible. With E12gc/ml titration, an almost linear correlation was observed between the volume of virus injected and the number of neurons transduced and the cortical volume of transfection. With E13gc/ml titration the correlation between the injected AAV volume and the number of neuronal transductions was still good but there was a poor correlation between AAV volume and transfection volume. We concluded that E12gc/ml titration was a more reliable option for our further studies. The reliability of E13gc/ml titration needs to be proven.

Table of contents

Table of Contents

List of figures

List of Abbreviations

AAV	Adeno-associated virus
BDNF	Brain-derived neurotrophic factor
CA1	Cornu Ammonis, first region of hippocampus
cAMP	Cyclic adenosine monophosphate
CNO	Clozapine-N-oxide
CREB	cAMP-response element binding protein (a cellular transcription factor)
DREADD	Designer receptor exclusively activated by designer drug
EEG	Electroencephalogram
EMG	Electromyogram
EOG	Electrooculogram
EPSP	Excitatory postsynaptic potential
FS	Fast spiking (interneuron)
GABA	Gamma aminobutyric acid
GAERS	Genetic Absence Epilepsy Rat from Strasbourg
G protein	Guanine nucleotide-binding protein
GPCR	G protein-coupled receptor
HSP	Homeostatic plasticity
hM3Dq	(Modified) human M3 muscarinic receptor activating Gq signaling
hM4Di	(Modified) human M4 muscarinic receptor activating Gi signaling
IL-1, IL-2	Interleukin-1 & 2
IPSP	Inhibitory postsynaptic potential
KA	Kainic acid
KD	Ketogenic diet
KORD	kappa-opioid receptor DREADD
LGN	lateral geniculate nucleus
miRNA	micro RNA
mRNA	messenger RNA
mTOR	mammalian target of Rapamycin
NTRK2	Neurotrophic receptor tyrosine kinase 2
PDS	Paroxysmal depolarizing shift
PSW	Polyspike-wave
PTZ	Pentylenetetrazole
PV	Parvalbumine
Pyr	Pyramidal
RE	Reticular thalamic nucleus
REM	Rapid eye movement
SE	Status epilepticus
SWS	Slow-wave sleep
TLE	Temporal lobe epilepsy
U/C	Undercut
W	Waking

Dedication

This work is dedicated to my wife, and to my mom for encouraging me to get into this endeavor and nursing me with affections and love and their partnership for success in my life

Acknowledgement

I would like to thank my supervisor, Dr Igor Timofeev, for giving me the opportunity to work in his tremendous laboratory, and for helping me in starting the fundamental neuroscience research.

I also appreciate Dr Sylvain Chauvette, lab's research assistant, who assisted in performing experiments at the beginning, and guide me with living issues in Canada.

I would like to thank Sara Soltani, PhD, who was very helpful in guiding me throughout my experiments, even though she was working as a post-doc fellow in another research centre.

I also thank my colleagues, PhD students, Anastasia Ozur, Diellor Basha, and Dr Richard Quansah Amissah, whose comments and assistance were very helpful to me.

A special thanks to Mr Sergiu Ftomov, lab technician, who was always there for providing technical assistance before, and during experiments.

Introduction

Traumatic brain injury can lead to devastating physical and social inabilities. It may also lead to epilepsy which consist of different diseases with a common feature: unprovoked seizures due to increased local network excitability. Different animal models have been designed to simulate traumatic brain injury (TBI) and posttraumatic epileptogenesis, of which the partial cortical deafferentation (undercut) mimics penetrating brain injury. In first part of this introduction, neocortical cytoarchitecture, neuronal excitability, the potential factors affecting epileptogenesis, and animal models of TBI will be reviewed, with special reference to the undercut model. The second part pertains to G protein coupled receptors (GPCRs), Designer Receptor Exclusively Activated by Designer drug (DREADDs), and the adeno-associated viral vectors (AAVs).

Normal cortical cytoarchitecture

The neocortex might be the result of a repeated duplication of a microcircuit template which is stereotypical and specialized as per brain region and in different species. Cerebral cortex comprises about 80% of human brain volume (Herculano-Houzel, 2012). Horizontally, neocortex is divided into six layers or laminae, from pial surface to the border with white matter. The neurons of superficial layers are younger than those of deeper layers in accordance to stages of embryonal development (Fame et al., 2011).

Layer I is essentially composed of apical dendrites of pyramidal neurons, a small number of GABAergic neurons, and lots of axon terminals (Douglas and Martin, 2004). Only layer I lacks pyramidal neurons (Ramaswamy and Markram, 2015).

Layer II/III contains the soma of 80% of callosal-projecting pyramidal neurons of which the majority lie in layer III (Porter and White, 1986; Fame et al., 2011). In primates, the layers II and III are distinct but in the mouse they are indistinguishable (Fame et al., 2011).

Layer IV consists of some different kinds of spiny neurons such as spiny stellate cells (Staiger et al., 2004) which mainly receive projections from thalamic neurons (Kaas, 2013).

Layer V comprises of pyramidal neurons and is home to 20% of callosal projection neurons (Fame et al., 2011). Layer V is divided into upper layer V (layer 5A) which consists of pyramidal neurons having slender apical dendrites and an axon projecting to the striatum and/or the contralateral hemisphere by coursing through the corpus callosum, and lower layer V (layer 5B) mainly composed of thick-tufted layer 5 (TTL5) neurons, mostly projecting to subcortical regions (Ramaswamy and Markram, 2015). This subcortical regions includes the striatum, brainstem and spinal cord nuclei (axons coursing through the pyramidal tract (Cowan and Wilson, 1994)), and ipsilateral pontine nuclei (Kita and Kita, 2012), and also to higher order thalamic nuclei (Van Horn and Sherman, 2007). Approximately 80% of collaterals that connect primary motor cortex to primary somatosensory cortex arise from callosal projection neurons in layers V and VI (Veinante and Deschenes, 2003).

Layer VI is an important input layer like layer IV, by receiving thalamocortical input, and a major output layer by sending projections to first order thalamic nuclei (Van Horn and Sherman, 2007) from about 30-50% of its pyramidal neurons, to cortex (corticocortical) via long horizontal axons, to claustrum, and to deep layers of cortex (Thomson, 2010).

Vertical structure of neocortex comprises neocortical minicolumns which are groups of synaptically linked neurons. These minicolumns are interconnected via short-range horizontal links to form cortical columns (Mountcastle, 1957, 1997). In each neocortical column of rodents, there are about 7,500 neurons (Ren et al., 1992; Beaulieu, 1993) but the number of cells in every layer is different:
Layer I: 100 neurons, Layer II/III: 2,150, Layer IV: 1,500, Layer V: 1,250Layer VI: 2,500.

Neocortical neurons are comprised of 70 to 80% excitatory pyramidal neurons (Peters and Sethares, 1991; DeFelipe and Farinas, 1992) and 20-30% of interneurons which predominantly contain the inhibitory neurotransmitter GABA (Markram et al., 2004). The excitatory pyramidal neurons comprise the major cortical neurons that exist in every neocortical layer with the exception of layer I. They share a similar morphology, but are slightly different in the size and shape of their soma, their dendritic arborization, the density of their spines, and their axonal projections

(DeFelipe and Farinas, 1992).

Common features of inhibitory interneurons

Morphology, physiology, synaptic and molecular features are different among interneurons (Cauli et al., 1997; Kawaguchi and Kubota, 1997; Gupta et al., 2000), but they have some common characteristics as well. Their dendrites are aspiny, and their soma may receive either excitatory or inhibitory synapses (Markram et al., 2004). They are local circuit neurons: the arborization of their neurites are confined to neocortex (Letinic et al., 2002). Their axons can synapse onto different regions of target neurons: soma, dendrite, or axon (DeFelipe, 1997; Somogyi et al., 1998).

Main states of vigilance

There are three main states of vigilance: Waking (W), slow-wave sleep (SWS) and rapid eye movement (REM) sleep. Interestingly, waking and REM sleep share similar characteristics of neocortical activity: persistent synaptic activity and neuronal firing. The SWS presents transitions between depolarization and hyperpolarization of neuronal membrane potentials (Steriade et al., 2001; Timofeev et al., 2001).

Electroencephalographic (EEG) characteristics of states of vigilance

Waking state: low-amplitude, high-frequency beta (13-25 Hz) and gamma (30-60 Hz) oscillations predominate, but there are also alpha rhythm (8-12 Hz) over visual cortex with the eyes closed (Compston, 2010), and mu rhythm (8-12 Hz) over somatosensory cortex during immobility (Rougeul et al., 1972; Rougeul-Buser et al., 1975; Bouyer et al., 1983).

SWS: mainly slow oscillations, but also fast components like spindles (sigma bursts of 12-15 Hz), beta and gamma oscillations and even ripples (>80 Hz) (Steriade, 2006).

REM sleep: waking-like activity in electroencephalography (EEG), total loss of muscle tone in electromyography (EMG) and fast ocular movements in electrooculography (EOG) (Luppi et al., 2013). Cortical neurons show depolarized membrane potential, and spontaneously fire (Steriade et al., 2001).

During SWS, because of a hyperpolarized silent state, the neuromodulatory system activity is the lowest when compared to waking and REM sleep, and neocortical seizures happen most often during SWS (Timofeev et al., 2013). Sleep

spindles are waxing-and-waning field potentials, lasting 1-3 seconds and repeating every 5-15 seconds (Timofeev and Bazhenov, 2005). There are two types of spindles, fast (12-15 Hz) and slow spindles (9-12 Hz) (Ayoub et al., 2013). Fast spindles originate from thalamus but it is unclear where the slow spindles are produced (Timofeev and Chauvette, 2013). Slow spindles' frequency is identical to fast runs (7-16 Hz), and they are both recorded from frontal cortical regions. So, slow spindles might be of cortical origin (Timofeev et al., 1998).

During seizures cortical neurons generate paroxysmal depolarization shift (PDS). PDS is the neuronal depolarization during paroxysmal EEG/LFP spikes (Timofeev et al., 2014). After PDS cortical neurons are hyperpolarized which is reflected as a wave component of EEG/LFP. This hyperpolarization is mediated by (a) disfacilitation, that is lack of synaptic activities, and (b) Na^+ and Ca^{2+} dependent K^+ currents (Timofeev and Steriade, 2004). The hyperpolarization during wave component of seizures activates h current. The h current is a depolarizing current that eventually leads to neuronal firing. When these subsets of neurons fire a new paroxysmal cycle starts. Paradoxically, during paroxysmal activities the IPSPs which depend on chloride are depolarizing while still being inhibitory. The reason is the inhibitory interneurons fire excessively and the extracellular K^+ concentration is high (Cohen et al., 2002; Timofeev et al., 2002), and the activity of the neurone-specific K^+-Cl^- cotransporter 2 (KCC2) results in a positive shift in Cl^- reversal potential (DeFazio et al., 2000).

Throughout sleep two mechanisms may potentially increase the likelihood of seizure activity: (a) during silent states, disfacilitation upregulates excitability of neurons through homeostatic plasticity; (b) during slow oscillation sleep synaptic excitability is increased with long-term potentiation (Timofeev et al., 2014).

Cortical origin of paroxysmal oscillations generated within the thalamocortical system

Such paroxysms exist in cortical neurons, in vivo as well in vitro (Timofeev et al., 1998), and can be induced by intracortical infusion of bicuculline ($GABA_A$ receptor antagonist), even after ipsilateral thalamectomy in cats (Steriade and

Contreras, 1998), whereas intrathalamic injection of bicuculline is not associated with spike-wave seizures in some studies (Ajmone-Marsan and Ralston, 1956; Castro-Alamancos, 1999). The work of Bal et al. showed some similarities between absence seizure and spike and wave seizures induced by bicuculline injections in the thalamic lateral geniculate nucleus (LGN) of ferrets (Bal et al., 1995). Thalamocortical and corticothalamic fibers are excitatory glutamatergic. Both of them send fibers to reticular (RE) thalamic nucleus. The neurons in RE are GABAergic and interconnected with gap junctions (Landisman et al., 2002; Fuentealba et al., 2004). Corticothalamic fibers excitatory conductance (quantal size) in RE neurones are 2.6 times greater than that of thalamocortical neurons (Golshani et al., 2001). Therefore, during these paroxysmal cortical activities, the thalamocortical neurons are predominantly hyperpolarized and so inactive (Pinault et al., 1998; Steriade and Contreras, 1998; Timofeev et al., 1998; Timofeev and Steriade, 2004).

Seizure cycle characteristics

Typically, most seizures begin with spike-wave--polyspike-wave (SW-PSW) complexes of 1-3 Hz with a gradual increase in PSW component that are replaced by the fast runs of 8-14 Hz (Figure I-1). Then a new transition to PSW occurs with a progressive decrease in spikes numbers and finally in SW discharges (Bazhenov et al., 2008). The spike components are mainly inhibitory (Timofeev et al., 2013).

Pathophysiology of seizures of cortical origin

Epileptic seizures are characterized by synchronized hyperexcitation of neurons in neuronal network and more specifically due to the driving force of extracellular K^+ on neural activity (Bazhenov et al., 2008). Lack of balance between excitatory and inhibitory neurotransmission has been considered as the main cause of seizures. (Dudek and Spitz, 1997; McCormick and Contreras, 2001).

POSTTRAUMATIC EPILEPSY

Neural circuit reorganization

Injury-induced epilepsy (in human and also in animal models) is characterized by brain plasticity and strongly linked to axon sprouting and neural circuit

reorganization. Due to the presence of recurrent excitatory axonal projections, the excitatory connectivity is increased, and the inhibition is less efficient. Many researchers considered these changes as the cellular basis for abnormal synchronous activity of neural network and seizures (Traub and Wong, 1982; Dudek and Spitz, 1997; McCormick and Contreras, 2001).

Excitatory circuit changes

Mossy fiber sprouting was first described in dentate gyrus following trauma. In this condition, dentate granule cells connect to each other through sprouting of axon collaterals reaching the inner molecular layer. This network acts as a recurrent excitatory substratum during epileptogenesis (Cronin and Dudek, 1988; Cronin et al., 1992; Wuarin and Dudek, 1996; Lynch and Sutula, 2000; Wuarin and Dudek, 2001; Winokur et al., 2004).

A few research groups have investigated these modified local mossy fiber connections in human (Sutula et al., 1989; Houser et al., 1990; Babb et al., 1991; Zhang and Houser, 1999) and in animal models of Temporal lobe epilepsy (TLE) (Nadler et al., 1980; Ben-Ari, 1985; Tauck and Nadler, 1985; Cronin and Dudek, 1988; Buckmaster and Dudek, 1997; Buckmaster et al., 2002; Shibley and Smith, 2002). Posttraumatic mossy fiber sprouting is more robust following severe TBI (Hunt et al., 2012) and is often limited to areas close to the injury. Both spontaneous and elicited burst discharges have been observed by single-cell and local field potential recordings from granule cells in post-TBI slices with mossy fibers, surgically isolated from afferent input coming from entorhinal cortex. This indicates a synchronous network activation (Hunt et al., 2009, 2010).

Intergranular cell connections, absent in the normal dentate gyrus, have been suggested to occur following TBI using localized glutamate stimulation of sprouted mossy fibers in slices (Hunt et al., 2010). Mossy fiber sprouting may provide a means for regional granule cell network synchronization after TBI that may be “unmasked” if inhibitory control is impaired (Patrylo and Dudek, 1998).

Similar changes have been seen after neocortical undercut that could be due to strengthened excitatory synapses onto pyramidal neurons of CA1 of hippocampal region (Prince et al., 2012). Salin et al. compared brain morphology of two groups of

adult rats, control and neocortical deafferented undercut group and observed the presence of axonal sprouting associated with epileptogenic recordings in undercut group. The intracortical connectivity was increased as a result of the increase in length and volume of axons and their branches and the increase in the density of axonal boutons (Salin et al., 1995). Kusmierczak et al. could show in deafferented cats an intracortical sprouting from the relatively intact cortex toward the damaged neocortex associated with an increase in horizontal connectivity of neuronal processes (Kusmierczak et al., 2015). Therefore, brain trauma of different areas triggers neuronal sprouting that could represent an important epileptogenic factor.

Inhibitory circuit changes

GABAergic interneurons exert a strong control on overall cortical activity. $GABA_A$ receptors (Figure I-2) perform inhibition through two mechanisms:

1) Phasic (synaptic): high concentrations of GABA release from the presynaptic membrane evoke a rapid transient activation of postsynaptic $GABA_A$ receptors. This phenomenon is believed to be restricted to the synaptic junction.

2) Tonic (extrasynaptic): low concentrations of GABA escaping the synaptic cleft persistently activate high affinity extrasynaptic $GABA_A$ receptors on the same neuron or the neurons in the vicinity (spill over).

After TBI, loss of ipsilateral inhibitory hilar neurons is linked to reduced synaptic (phasic) inhibition of granule cells (Hunt et al., 2011; Pavlov et al., 2011; Gupta et al., 2012). There are also reductions in expression of $GABA_A$ receptor subunit (Mtchedlishvili et al., 2010; Gupta et al., 2012; Raible et al., 2012). Different groups reported unidentical changes in tonic inhibition: increased in contralateral dentate granule cells (Mtchedlishvili et al., 2010), with no change (Pavlov et al., 2011) or even markedly decrease (Gupta et al., 2012).

In the undercut model of cortical deafferentation, layer V fast spiking (FS) interneurons receive fewer connections from presynaptic interneurons. The cause might be a decrease in the number of interneurons, diminished total length of interneurons axonal arbors, reduced number of GABAergic synapses, or decreased probability of synaptic GABA release onto pyramidal and FS cells. A reduction in the

number of axonal boutons of FS interneurons can decrease inhibitory drive to layer V pyramidal neurons (Jin et al., 2011).

Homeostatic plasticity

Homeostatic plasticity (HSP) (Turrigiano, 1999) is a set of the synaptic and intrinsic mechanisms in order to preserve a normal level of neuronal activity. Synaptic scaling takes place partly at postsynaptic level through changing the glutamate receptor numbers (Rao and Craig, 1997; Lissin et al., 1998; O'Brien et al., 1998; Turrigiano and Nelson, 1998; Watt et al., 2000; Liao et al., 2001), and at presynaptic level through changes in neurotransmitter release probability (Murthy et al., 2001). There is also a decrease in number of $GABA_A$ receptors at synaptic level (Kilman et al., 2002). Chronic blockade of activity results in an increase in Na^+ currents and a decrease in K^+ currents, and the sum is an enhanced responsiveness of pyramidal cells to current injections (Desai et al., 1999).

Deafferented cortex

Acutely isolated cortex may generate slow oscillations similar to what is produced by an intact cortex during sleep while completely deafferented neocortical slabs may initially be unable to produce slow oscillations until after a two-week period, due to the absence of corticocortical excitatory connections (Lemieux et al., 2014). There could be a common mechanism of the slow oscillations and the spontaneous bursts in chronically deafferented cortex, which is directly proportionate to the power of recurrent excitatory synaptic connections (Houweling et al., 2005).

The effect of HSP is different after partial vs complete deafferentation

Homeostatic synaptic plasticity is a mechanism for restoring network activity when insults perturb this activity. Nearly complete cortical deafferentation leads to slow oscillation network activity. In contrast, after partial deafferentation, homeostatic plasticity restores a normal asynchronous state. This results from upregulation of pyramidal cells intrinsic excitability alone (Houweling et al., 2005). However, it has been shown that partial cortical deafferentation is a potent epileptogenic factor (Topolnik et al., 2003b). Therefore, homeostatic plasticity is a major mechanism of posttraumatic epileptogenesis. Brain-derived neurotrophic

factor (BDNF) prevents the homeostatic plasticity of excitatory and inhibitory synapses (Rutherford et al., 1997; Rutherford et al., 1998) in cell cultures.

HSP in young animals

In young animals the upregulation process is halted (Figure I-3) when physiological levels of excitability are achieved but in adult animals the process to detect this upper limit of excitability (possibly through a sensor) is dysfunctional. This uncontrolled excitability in adult can lead to cortical epilepsy (Timofeev et al., 2013).

EPILEPTOGENESIS

«The term “epileptogenesis” refers to a transformation process by which the normal brain develops an increased propensity for generating spontaneous seizures» (Lothman et al., 1991)

«This process typically involves structural alterations in neural circuitry due to progressive neuronal damage and “self-repair” mechanisms–which develop through a latent period of variable time and culminate with the emergence of spontaneous, recurrent, seizures» (Dudek and Spitz, 1997).

The frequency and severity of spontaneous recurrent seizures show a sustained increase after the first seizure (Bertram and Cornett, 1993; Bertram and Cornett, 1994; Hellier et al., 1998; Nissinen et al., 2000; Williams et al., 2009; Kadam et al., 2010).

Mechanisms of epileptogenesis

1. Cellular and network mechanisms excitatory positive feedback through:

a) Damage to inhibitory neuron circuitry can unmask the normal positive feedback (Shao and Dudek, 2005) and increase the net functional positive feedback in epilepsy (Cronin et al., 1992)

b) Sprouting of new synaptic connections between surviving, deafferented neurons after TBI (Tauck and Nadler, 1985; Cronin et al., 1992; Wuarin and Dudek, 1996; Sutula and Dudek, 2007; Buckmaster, 2012).

Seemingly, provided the sprouting is predominantly GABAergic or glutamatergic onto interneurons (Babb et al., 1989; Zhang et al., 2009), this could be a strong antiepileptogenic mechanism. However, Jin et al. showed a reduced inhibitory connectivity to both FS interneurons and pyramidal cells in undercut model

with an increased excitatory connectivity to pyramidal cells. The result is epileptogenic activity (Jin et al., 2011).

2. Molecular mechanisms

Most of the omics studies (analysis of transcriptome, epigenome, proteome, or metabolome) in epileptogenesis pertain to gene expression (microarrays, and sequencing technologies):

Transcription factors can control expression of many genes. Examples are inducible cAMP early repressor (ICER) that supresses kindling (Kojima et al., 2008; Porter et al., 2008), cAMP response element (CREB) which controls differential expression of genes in human epileptic cortex (Beaumont et al., 2012), and repressor element-1 silencing transcription factor (NRSF) that can repress epileptogenesis in a kindling model and can also regulate target genes appropriate for neuronal network remodeling in kainate-induced SE (Hu et al., 2011; McClelland et al., 2014).

Epigenetic regulation can be achieved through alteration in DNA methylation (Kobow et al., 2013) or histone modifications, or by transcriptional regulation via micro-RNAs (miRNAs). In animal models of epileptogenesis some micro-RNAs are commonly found: miR-146a which regulates the astrocyte-mediated inflammatory response is upregulated in activated astrocytes during epileptogenesis (Aronica et al., 2010; Iyer et al., 2012; Jovicic et al., 2013). miR-132 that increases dendritic outgrowth and arborization and is involved in spine density regulation is upregulated in neurons during epileptogenesis (Jovicic et al., 2013). miR-21 and miR-34a have also been found in animal models of epileptogenesis (Pitkanen et al., 2015).

Cell proliferation and plasticity

Neurotrophins concentrations are raised in experimental and adult epileptic tissue. Brain-derived neurotrophic factor (BDNF) might be involved in human epilepsy (Scharfman, 2005). Conversely, there are studies indicating that BDNF prevents homeostatic plasticity (see above). Neurotrophic tyrosine kinase receptor type 2 (NTRK2) regulates excitability in vivo in mice. Erythropoietin shows neurotrophic effects. It plays also a role in signaling antiapoptotic, antioxidant, anti-inflammatory functions. Erythropoietin reduces frequency and duration of seizures by reducing blood-brain barrier (BBB) damage, neurodegeneration, microglial

activation, development of ectopic hilar granule cells, gliosis (Chu et al., 2008)

Inflammatory cell adhesion

Integrin α4/β1 and P-selectin glycoprotein ligand 1 mediate leucocyte adhesion to brain vascular endothelial cells following pilocarpine-induced SE. Only seizure frequency could be reduced with integrin-α4-specific monoclonal antibody (α4 MAb) but the latency and duration of seizures did not change. However, there was less severe BBB damage at the acute phase (18-24 hours post-SE) and a reduction in chronic neurodegeneration (30 days post-SE) in mice treated with a4 Mab (Fabene et al., 2008).

Protein kinase

Mammalian target of rapamycin (mTOR) controls protein synthesis and cell growth through downstream effectors such as p70 ribosomal S6 kinase1 (S6K1). Phosphorylated S6k1 phosphorylates ribosomal protein S6, which will promote production of ribosomal proteins and elongation factors in order to increase translation (McDaniel and Wong, 2011). mTOR may contribute to epileptogenesis through a) induction of IL-2 mediated T-cell proliferation causing inflammatory reactions that lead to injury, or b) aberrant axonal sprouting and neurogenesis (because of its role in neuronal development and plasticity).

Phosphatase and tensin homolog (PTEN) is a tumor suppressor upstream of mTOR that inhibits phospho-inositide 3-kinase (PI3K) activity, and PTEN mutation results in mTOR hyperactivity (McDaniel and Wong, 2011).

During SE induced by KA, mTOR is activated in cortex and hippocampus, and after 24h backs to normal level. During the latent period 5-7 days after SE, mTOR elevates again only in hippocampus. Status epilepticus results in widespread glutamate release, and glutamate NMDA (N-methyl D-aspartate) receptor activation in turn can stimulate mTOR through the PI3K/Akt (Akt: protein kinase B) signaling cascade. Phosphorylation of Akt accompanies both the early and late mTOR activation after KA-induced status epilepticus, and indicates implication of PI3K signaling in epileptogenesis in this model (Zeng et al., 2010). Overactivation of NMDA receptors in the KA model causes calcium influx that activates calcium-

dependent neuronal death pathways. Rapamycine administered before KA, through inhibition of mTOR, induces autophagy that might prevent neuronal death and epileptogenesis by enhancing cell survival during increased metabolic demand of SE.

Curcumin may represent a new class of mTOR inhibitor which can suppress epileptogenesis in animal models of epilepsy (Beevers et al., 2009; Jyoti et al., 2009). The ketogenic diet (KD) is a high-fat, adequate-protein, low-carbohydrate diet that is an effective treatment for some forms of epilepsy (Hemingway et al., 2001; Marsh et al., 2006; Neal et al., 2008; Patel et al., 2010). The KD reduces insulin levels (Thio et al., 2006) which could decrease PI3K/Akt signaling and inhibit mTOR activity.

Neurotransmitter receptor: fragile-X syndrome

In murine model with knockout for Fmr1 gene, there is dendritic spine density and susceptibility to audiogenic seizures. The silencing in dendritic mRNA of group I metabotropic glutamate receptor (mGluR1) could generate the seizure. But a co-reduction in mGluR5 expression restores the majority of aberrancies in the structure and function such as dendritic spine density and seizures (Dolen et al., 2007; Qiu et al., 2009).

The Role of Sirt1 in Epileptogenesis

Silent information regulator 2 proteins [sirtuins (Sirts)] are a class III histone deacetylase that require nicotinamide adenine dinucleotide (NAD+) for their enzymatic activity as a protein deacetylase (Blander and Guarente, 2004; Herskovits and Guarente, 2014). This majorly nuclear protein is involved in gene transcription by deacetylating histones, in response to cellular energy demand (Canto and Auwerx, 2012; Srivastava, 2016)

Sirt1 may also play a regulatory role in metabolism, apoptosis, autophagy, and mitochondrial function. Sirt1 upregulation occurs in epileptic patients (Chen et al., 2013), and in rat models of trauma-induced epilepsy (Chen et al., 2013; Wang et al., 2015; Brennan et al., 2016).

EX-527 is the antagonist of Sirt1 through competition for its NAD+ binding site and thus can prevent KA-SE-induced Sirt1 activity.

Mechanisms of inflammation-mediated hyperexcitability

1. Pro-inflammatory cytokines can modulate the receptors of neurotransmitters at neuronal membrane. For example, astrocytic TNF-α (tumor necrosis factor-alpha) increases synaptic expression of AMPA receptors lacking GluR2 subunit which means they are more permeable to Ca^{2+} that leads to synaptic strength through increased mEPSPs frequency (Beattie et al., 2002). TNF-α also reduces mIPSPs by inducing $GABA_A$ receptor endocytosis (Stellwagen et al., 2005).
2. Increased extracellular glutamate concentration by a) a reduced astrocytic reuptake of glutamate, b) inhibition of glutamine synthetase in astrocytes c) induction of glutamate release from glia (Ravizza et al., 2011).
3. COX-2 and PGE2: their inhibition can reduce neuronal excitability. They may reduce potassium currents in neurons. Free radicals produced during COX-2 synthesis of prostaglandins may promote glutamate-induced hyperexcitability (Ravizza et al., 2011).

Despite ineffectiveness of most anti-inflammatory studies, celecoxib in rats decreased the seizure frequency and duration. It was also associated with reduced hippocampal neurodegeneration and microglial activation, and inhibition of hilar ectopic granule cells formation and new glia in CA1 (Jung et al., 2006).

4. Increased blood-brain barrier permeability (Figure I-4) by IL-1 and TNF-α (Ravizza et al., 2011).
5. Long-term transcriptional effects: cytokines mediate cell death, neurogenesis and synaptic reorganization which occur during epileptogenic process (Ravizza et al., 2011).

Animal models of epileptogenesis

1) Injection of blood products inorganic iron salts, hematin and hemoproteins induce peroxidation of microsomal and mitochondrial lipids. They also alter the function of cellular thiodisulfide (Smith and Dunkley, 1962; Willmore and Ueda, 2009). Alpha-tocopherol and selenium could prevent this peroxidative reactions (Willmore and Rubin, 1981, 1984).

2) Kindling repeated subthreshold stimulation can induce the occurrence of generalized seizures (Kojima et al., 2008). Kindling is a plasticity phenomenon

leading to seizures which is in turn caused by subthreshold electrical, chemical, optogenetic stimulation (Goddard et al., 1969). Kindling is a model of epileptogenesis that is often investigated (Kandratavicius et al., 2014). It is a robust and reproducible tool for studying epileptogenesis (Sutula, 2004), but is costly and timely and the chronic implants may be lost (Kandratavicius et al., 2014).

3) Fluid percussion injury a pendulum hammer applying a mechanical force to a fluid- filled cylinder which in turn transmits the pressure to brain in a craniotomized animal. This method simulates closed-head traumatic brain injury and is histologically associated with mossy fiber sprouting and ipsilateral hippocampal atrophy (Hunt et al., 2013). With midline craniotomies the injuries are more diffuse while lateral craniotomies are associated with mixed focal and diffuse injuries (Rowe et al., 2016).

4) Weight drop (impact-acceleration) injury dropping a weight impacts rat skull. Cortical and subcortical injuries are extensive and includes dentate gyrus and hippocampus. Spontaneous seizures have not been observed in this study model but increased susceptibility to pentylenetetrazole (PTZ) 15weeks after injury were reported (Golarai et al., 2001).

5) Controlled cortical impact injury mostly performed by using a pneumatic impactor which is controlled electronically to induce a focal brain injury through craniotomy. Despite weight drop and fluid percussion injuries, this model produces a relatively consistent and reproducible focal injury and reduces inaccuracy and the risk of rebound injuries. Seizure onset as early as 24 hours were reported, in rats (Nilsson et al., 1994; Kochanek et al., 2006) and mice (Hunt et al., 2009).

6) Blast injury mimicking ballistic penetrating injury in war. A water balloon is rapidly inflated and deflated by a hydraulic pressure generator. This creates a cavity in neocortex. 70 percent of the animals in this study developed seizures 72 hours after injury (Hunt et al., 2013).

7) Withdrawal of chronic GABA infusion Paroxysmal activity occurs upon discontinuation of GABA infusion in vivo in baboons (Brailowsky et al., 1987) and in rats (Brailowsky et al., 1990) and in vitro in rats (Calixto et al., 2000). The seizure

activity might be due to a downregulation of $GABA_A$ receptor in neurons in response to a high concentration of GABA (Tehrani and Barnes, 1988).

8) Partial cortical isolation causes hyperexcitability There is reorganization of cortical regions, altered GABAergic inhibition, increased frequency of EPSPs. Fast-spiking interneurons have high density of NaK ATPase. Brain derived neurotrophic factor (BDNF) from pyramidal cells act on tyrosine kinase receptor B (TrkB) in order to maintain connectivity but there is a reduced TrkB immunoreactivity of fast-spiking interneurons (Li et al., 2011).

9) Chemoconvulsants kainic acid (KA), analog of L-glutamate, as the rodent model of TLE. It triggers hippocampal seizures and causes injuries limited to hippocamus (Sharma et al., 2007). Pilocarpine, an agonist of muscarinic acetylcholine receptors, causes injuries in hippocampus, as well in neocortex. It models TLE better than KA and causes limbic seizures (Furtado et al., 2011). Chemoconvulsants were used to elucidate acute seizures but not epilepsy (chronic conditions). Other widely used chemoconvulsants are pentylenetetrazole (PTZ) causing absence or myoclonic seizures, strychnine, N-methyl-D, and L-aspartate, all three generate generalzed tonic-clonic seizures (Loscher, 1997), penicillin, tetanus toxin, which may cause chronic epilepsy (Barkmeier and Loeb, 2009). PTZ has been used as a standard seizure test in most of antiepileptic drug trials (Loscher, 2017).

10) Genetic animal models genetic epilepsies in mice and other animals may be spontaneous or engineered (Grone and Baraban, 2015). Two examples are DBA/2 mice presenting audiogenic seizures (Loscher, 2017), and Genetic Absence Epilepsy Rat from Strasbourg (GAERS) (Danober et al., 1998). These models are mostly used to develop antiepileptic drugs (Vergnes et al., 1982).

The question about usefulness of animal models is raised because of numerous failures especially when applying in humans as clinical trial. The reasons could be: inappropriate animal model, inability to check some methods in humans (such as kindling), lack of uniformity of different models (Willmore, 2012).

The neocortical undercut model

To study posttraumatic hyperexcitability and epileptogenesis, the undercut (U/C) model which is similar to a penetrating brain injury is useful. It consists of

cutting the cerebral cortex (particularly the sensorimotor cortex) and the white matter that lies underneath it (undercut), so that a large cortical region is isolated not only from the neighboring cortex but also from subcortical regions (Hoffman et al., 1994; Topolnik et al., 2003a).

If undercut is done during the first week of life only a thinned white matter and overlying cortex may be seen. After this period, undercut lesion is more elusive in term of indicating a border between cortex and white matter (Prince and Tseng, 1993). Microscopic examination of the same slices elucidated loss of cortical thickness and decrease in number of cells in infragranular layer where shrunken dark-staining pyramidal neurons were present (Prince and Tseng, 1993).

In the rat, partial neocortical isolations indicate that layer V PV-containing fast spike (FS) interneurons show changes in their axonal terminals and dendrites, but their numbers remain almost the same (see next paragraph). In infragranular Pyr cells decrease in soma size. In the undercut cortex, there are marked reductions in intensity of perisomatic halos of vesicular GABA transporter (VGAT-), glutamic acid decarboxylase (GAD65-, and GAD67)-IR (Gu et al., 2017). The analysis of biocytin-filled boutons and electron microscopy show that modifications in halos intensity could be due to decreased expressions of these GABA markers in each bouton, and a reduction in inhibitory synapses (Gu et al., 2017).

The onset of changes in suprasylvian gyrus of cats following deafferentation was seen as early as 2 weeks after transecting the fibers in the white matter but are more prominent at 4 weeks and 6 weeks (Figure I-5). These changes include disarray of normal distribution of cells in layers and columns, with severe cell loss in deep layers of suprasylvian gyrus and dystrophy of remaining cells, i.e., small atypical and pycnotic nuclei. In addition, a reduction in the cortical gray matter thickness is observed, that is, from 1.87±0.17mm in control animals to 1.72±0.16mm, 1.5±0.21mm, 1.45±0.18mm at 2, 4 and 6 weeks, respectively (Avramescu et al., 2009).

The number of both non-GABAergic (presumed as excitatory), and GABAergic neurons decreases in deep layers V and VI, but also in more superficial layers II and III, but the reduction in inhibitory neurons is far more noticeable compared to

excitatory neurons (Avramescu et al., 2009).

The focus of epilepsy is a specific region of the cerebral cortex characterized by a remarkable damage caused by different kinds of pathologies. The focus of seizure is the area surrounding the epileptic focus and is composed of highly excitable neurons that can trigger seizures. In the undercut model, the focus of epilepsy is the undercut area whereas the seizure focus lies around the undercut cortex (Timofeev et al., 2014).

U/C Increases excitability

According to electrophysiological observation (Li and Prince, 2002), following undercut the following changes are expected in layer V: an increase in AMPA-receptor-mediated excitation, a decrease in $GABA_A$-receptor-mediated inhibition, an impaired chloride homeostasis, and newly formed recurrent excitatory circuits

The sum of these modifications may increase synaptic excitation and thus play a role in epileptogenesis (Jin et al., 2006). Layer V FS interneurons received a significantly increased excitatory and a decreased inhibitory synaptic connectivity in undercut mice. In epileptogenic rats, there was a marked decrease in inhibitory synaptic connectivity towards layer V pyramidal neurons. There is also up-regulation of intrinsic excitability (see below).

The advantages of the undercut model

The main advantages of the undercut model are easy preparation, high reproducibility, and low animal mortality (Jin et al., 2011). Epileptiform activity in this model is high (95%) in vitro and a good percentage of living animals. Additional advantages include reduced variability by a more localized and consistent lesion. This model provides efficient approach to study epileptogenesis and factors implicated with its pathological process, including axonal sprouting, HSP, changes in excitatory and inhibitory circuits (Jin et al., 2011).

Limitations of the undercut model

There is no major physical impact as opposite to TBI or most of other models of brain trauma. In traumatic brain injuries there are injuries to remote structures, such as hippocampus, as well, whereas in the undercut model only a limited injury is produced (Jin et al., 2011).

Seizure in undercut cortex

In the undercut cortex of cats anesthetized with ketamine-xylazine, in acute conditions, the silent states are longer in cortex over undercut region as compared to normal cortex (Topolnik et al., 2003b). Even without anesthesia, more silence was reported (Timofeev et al., 2010). The characteristic feature of seizure onset is the shortening of active and silent phases, associated with a slightly increased depolarization amplitude only during active states. In the main part of a seizure, there is a slight hyperpolarization followed by a prominently increased amplitude during PDS (Topolnik et al., 2003a).

The duration of acute paroxysmal activity was 8-10 h. Seizures always started in areas surrounding the undercut (Topolnik et al., 2003a). These seizures were likely caused by immediate trauma effects, such as increased extracellular K^+ and increased glutamate etc. In chronic conditions, spontaneous seizures restarted several days/weeks later (Nita et al., 2007; Timofeev et al., 2013; Ping and Jin, 2016). In fact, in this area, despite what happened to undercut microstructure, there was much less GABAergic neurons loss (Avramescu et al., 2009).

Following cortical partial deafferentation, a vicious cycle is formed: axonal sprouting increases the network synchronization, which leads to seizure and paroxysmal activity in undercut cortex that directly reinforces sprouting. Therefore, a partial cortical isolation is accompanied by increased number and duration of silent states in cortical networks leading to boosted neuronal connectivity and network excitability.

Intrinsic excitability changes in the undercut model

Acute condition: neuronal membrane potential in deafferented cortex is more hyperpolarized as compared to that of surrounding cortex. The misbalance in excitability between these two neighboring areas is the leading cause of acute seizures (Topolnik et al., 2003b). The possible reason for a high firing rate of neurons is a high extracellular K^+ resulting from cell damage (Jensen et al., 1994; Jensen and Yaari, 1997).

Chronic conditions: as early as the second week after performing undercut, there is an increase in the input resistance of neurons and their instantaneous firing rate.

The intrinsic and synaptic excitability changes are the causes of a prolonged silent state, which in turn is compensated by increased instantaneous spontaneous firing rates (Avramescu and Timofeev, 2008).

Changes in synaptic excitability in the undercut model

After undercut, there is a reorganization in neocortical synapses due to axon sprouting. Layer V pyramidal neurons get more excitatory synaptic connectivity after undercut (Jin et al., 2006). There is also a reduced inhibitory synaptic connectivity onto layer V pyramidal cells. The FS interneurons in layer V of mice neocortex receive more excitatory and less inhibitory synaptic connections compared to natural situations. In undercut cortex, pyramidal neurons of layer V form a recurrent excitatory connection with other pyramidal cells of layer V and with FS interneurons as well. Layer V FS interneurons regulate network excitability at intralaminar level (Jin et al., 2011). It seems that any synaptic input onto intact cortical neurons near undercut can generate marked depolarizations that could lead to seizures (Topolnik et al., 2003a). While in acute posttraumatic period, there is a failure in synaptic transmission, an increased excitatory synaptic connectivity is observed after chronic cortical deafferentation. The characteristic feature of this excitatory synaptic efficacy is an increase in amplitude accompanied by a reduced duration particularly at 2 and 6 weeks after undercut in cats (Avramescu and Timofeev, 2008). Following penetrating brain injury, glial cells activate and predispose the neocortex to axonal sprouting and forming new synaptic connectivity among neurons survived from acute injury. The duration of silent states increases in the cortical network because of a reduced number of neurons. The overall result is the activation of homeostatic plasticity to restore a normal activity by increasing excitability in remaining network neurons (Timofeev et al., 2010).

G protein-coupled receptors (GPCRs)

GPCRs comprise the major group of membrane proteins. They can mediate different physiological responses via binding to a large number of ligands including metabolites, neurotransmitters, hormones. GPCRs also play an important role in olfaction, taste, and vision (Weis and Kobilka, 2018).

Following binding of ligands to GPCRs, the concentration of secondary messengers changes because of the activation of Gα subunits: Gαs upregulates cAMP production, Gαi inhibits production of cAMP, and Gαq leads to accumulation of Ca^{2+} (Yasi et al., 2020).

There are two types of GPCR signaling: *Canonical*, when a ligand binds to extracellular site of a GPCR, these receptors show a conformational change (Figure I-6), and their intracellular part couples to its effectors such as G proteins or β-arrestin. Then, through secondary messengers like Ca^{2+}, cAMP, or kinase, the downstream signaling cascade starts, and *noncanonica*l, when signaling is biased, associated with formation of oligomeric complexes, or originate from intracellular compartments (Shchepinova et al., 2020).

Biased signaling: according to the chemical structure of a ligand, only particular subgroups of a GPCR functional repertoire are activated (Smith et al., 2018). Biased drugs may provide a more precise pharmacological response (Tan et al., 2018).

GPCR oligomerization: The majority of GPCRs produce macromolecular complexes. These homo- or hetero-oligomer complexes are made up of two or more GPCRs (Gomes et al., 2016). Despite monomeric GPCRs, these oligomeric complexes can modulate (improve) some properties such as binding to ligands, bias signaling, and trafficking (Gomes et al., 2016; Botta et al., 2020).

GPCR compartmentalization: in addition to plasma membrane, the membranes of some other intracellular compartments are also implicated in GPCR signaling. These compartments comprise very early (Sposini et al., 2017), and early endosomes, the Golgi network, mitochondria, and nucleus (Jong et al., 2018; Ribeiro-Oliveira et al., 2019). This may provide new pharmacological targets (Thomsen et al., 2018).

Designer receptors exclusively activated by designer drugs (DREADDs)

Chemogenetics is a method of engineering proteins to make them capable of interacting with small molecule chemical actuators which have been unrecognizable by them naturally (Sternson and Roth, 2014). Designer Receptors Exclusively Activated by Designer Drugs (DREADDs) (Armbruster et al., 2007) are the most widely used class of chemogenetically engineered proteins. This is a chemogenetic

approach to noncanonical GPCR signaling to create agonists or antagonists of a given GPCR according to its signaling bias (Islam, 2018). An example is using the muscarinic DREADDs to selectively activate specific signaling patways: Gi, Gs, Gq, or β-arrestin (Roth, 2016).

Different types of DREADDs

Excitatory Gq-DREADDs the original DREADDs were based on human muscarinic receptors: hM1Dq, hM3Dq, hM5Dq. All 3 enhance neuronal firing via mobilizing intracellular calcium (Armbruster et al., 2007). hM3Dq is the most frequently used. CNO, an inert metabolite of clozapine, is the prototype actuator of these Gq-DREADDs. Usual dose of CNO is 0.1–3 mg/kg. CNO is back-transformed to clozapine (Jann et al., 1994) which in rodents is not negligible (Manvich et al., 2018). To activate DREADDs, low doses of CNO are used in order to get a transient peak activation and a fast decay of activity (Roth, 2016). It has been shown by different research groups that by locally applying CNO in DREADD-expressed brain regions, one can observe about 60% change in neuronal activity, that means increase in activity with excitatory and decrease in activity with inhibitory DREADDs (Gremel and Costa, 2013; Vazey and Aston-Jones, 2014; Chang et al., 2015). Alternatively, compound 21 (Jendryka et al., 2019) or Perlapine can be used but they need high systemic doses which may have some off-target effects (Thompson et al., 2018). More recently, deschloroclozapine (DCZ) has been used as a DREADD agonist with much higher affinity and potency for muscarinic DREADDs (Nagai et al., 2020).

Inhibitory Gi-DREADDs hM2Di, hM4Di, and KORD. The first two can be activated by CNO, compound 21, or Perlapine. The most commonly used is hM4Di.

k-opioid-derived DREADD (KORD) is activated by salvinorin B, a pharmacologically inert compound but a potent k opioid receptor agonist, is the synthetic form of salvinorin A (Wang et al., 2008).

The inhibitory effect of hM4Di and KORD is exerted through hyperpolarization induced by Gβ/γ-mediated activation of G-protein inwardly rectifying potassium channels (GIRKs) (Armbruster et al., 2007; Vardy et al., 2015) or inhibiting presynaptic release of neurotransmitter (Stachniak et al., 2014).

Modulatory Gs- and β-Arrestin-DREADDs by combining β-adrenergic receptor of turkey erythrocyte with a rat M3 DREADD the GsD was created. It has only a modest activity in transfected cells (Guettier et al., 2009) by activating cAMP production (Wang and Zhou, 2019).

The β-arrestin-specific M3 DREADD (Rq(R165L) recruits arrestin, instead of secondary messengers, for signaling cascade pathway following CNO binding (Nakajima and Wess, 2012).

DREADD expression

The time needed for DREADDs expression after injection of AAV viral vector is between 2-3 weeks in cell body, and 4-9 weeks in order to visualize anterograde pathways (axon, boutons, and synapses). Constructs composed of DREADDs and fluorophores or reporters, such as mcherry can help in localizing DREADDs, but the fluorophore expression depends on DREADD receptor regulation by the cell. The lower fluorophore expression makes current systems less efficient for morphological studies that rely on fluorescence intensity. Some reporters are readily visible by using filter cubes of fluorescent microscopes. These includes mcherry, EGFP, and EYFP (Smith et al., 2016).

Diminishing DREADD expression

DREADD expression of infected cells can be reduced by lowering the titer of virus, using a weaker promoter or modulating post-transcriptional expression (Roth, 2016). Repeated dosing of an agonist with a DREADD can lead to GPCR desensitization and internalization and downregulation (DeWire et al., 2007). The degree of desensitization depends on two factors: (1) receptors overexpression, (2) receptor reserve. Receptor reserve is defined as obtaining the maximum agonist response with activation of a small fraction of receptors (Ruffolo, 1982). Because only a small percentage of receptors are occupied, downregulation or internalization of receptors will not happen. As a result, when DREADDs are expressed through viral delivery or transgenically, we do not expect an important desensitization (Alexander et al., 2009; Krashes et al., 2011; Roth, 2016).

Seizure control with DREADDs

DREADDs may control seizures either by inhibiting the excitatory cells with hM4Di (Lieb et al., 2019), or by activating the parvalbumin positive interneurons with hM3Dq, which suppress epileptiform synchronization (Zhou et al., 2019).

Adeno-associated viral vectors (AAV's)

AAV's are small, single-stranded DNA viruses belonging to parvovirus family (Berns and Giraud, 1996). Their genome contains inverted terminal repeats (ITRs) which is important in synthesis of the second DNA strand through host cell DNA polymerase (Qiu and Pintel, 2008). To date, eleven serotypes of AAVs have been identified. The variable capsid structures make the difference in tropism among the serotypes (Agbandje-McKenna and Kleinschmidt, 2011). Pseudotyping is a recombination process in which different AAV serotypes are used to make a new capsid. This can increase AAV tropism for some cells and enhance transduction in neurons (Grimm and Kay, 2003; Sonntag et al., 2011). An example is AAV-DJ and its revised version AAV-DJ8 which are composed of 8 capsid types (Lerch et al., 2012).

When AAV adheres to the cell membrane, it may enter the cell via receptor-mediated endocytosis and endosomal trafficking (Ding et al., 2005). In the absence of a helper virus (adenovirus or herpes simplex virus), AAV cannot replicate and its genomes stay in a latent state in the form of an episome in the nucleus (Berns and Linden, 1995). Therefore, in constructs of AAV transfer plasmids, in addition to promoter, a helper virus genes are also contained to allow replication of AAVs (Grieger and Samulski, 2005). AAVs, like lentiviruses, may infect both dividing and non-dividing cells. In contrast, retroviruses can only infect dividing cells (Grieger and Samulski, 2005).

Advantages of using AAVs in neuroscience

AAVs are non-pathogenic, cause fewer immune reactions as compared to other viral vectors, can target neurons even without helper viruses or capsids, basal cell function is less affected by AAVs than with other vectors (Lentz et al., 2012).

Limitations of AAV usage

Low packaging capacity: AAV cannot carry large genes (Dong et al., 1996). AAVs have ssDNA genome and so they are dependent on host cell's replication assets for synthesis of the complementary strand (Haggerty et al., 2020). Serotype 2 (AAV2) is often used in neuroscience because of its natural tropism for neurons but it cannot transduce a large number of cells and presents a limited spread in a given brain region. The serotypes with a strong tropism for neurons, in vivo, are AAVs 1,2,5,7,8,9 (Castle et al., 2016).

The majority of AAVs may be transported anterogradely (from nucleus to axon and then to nerve terminals) but most of them are not suitable for retrograde transport (from nerve terminals to axon and then translocated in the nucleus) (Salegio et al., 2013). AAV1 and AAV9 can migrate through synapses and transduce a circuit network (Zingg et al., 2017).

Viral Promoters

Viral promoters enhance the expression of viral vectors in cells. There are two kinds of promoters: ubiquitous, in which expression in majority of cell types is high-level and longterm, and type-specific promoters that increase expression in some cell types (Haery et al., 2019). Some different promoters used in neuroscience are the human synapsin 1 gene promoter, the rat NSE gene promoter, the human U1 snRNA promoter, and the human cytomegalovirus. Among them only synapsin targets neurons but others target glial cells instead (Kugler et al., 2003). Synapsin is neuron-selective and not neuron-specific (Huda et al., 2014; Jackson et al., 2016), it can also increase expression in hepatocytes. The CBA promoter is stronger than synapsin but enhances expression in astroglial cells and in cardiomyocytes as well (Jackson et al., 2016). Therefore, synapsin is a better promoter for expression in neurons. Roughly, about two third of neurons express the DREADD receptor when synapsin-AAV8 is used (Smith et al., 2016).

AAV Titration

A functional vector titer is defined as the number of viral particles in a given volume that are required to infect a cell. The best way to measure the number of this functional particles is to use quantitative polymerase chain reaction (qPCR) in order

to quantify the number of viral DNA copies in each cell (Lizee et al., 2003). This can be performed by measuring capsid protein or the AAV genome, expressed in gene copies per milliliter (GC/ml) or viral particles per milliliter (VP/ml) (Wang et al., 2020). Multiplicity of infection (MOI) in a culture is the ratio of infectious virions to cells. The absence of infection means MOI equal to 0 while the virus may be present (Shabram and Aguilar-Cordova, 2000). Plaque-forming units (PFU) are the infectious virus titer measured by quantifying the plaques which upon infection with a given virus serial dilutions are formed in cell culture (Harcourt et al., 2020). The number of transducing units (TU/ml) is mostly used for lentivirus to quantify functional vector particles that lead to the expression of a fluorescent reporter protein.

Chapter 1 Hypothesis

General objective and hypothesis

It is known that in partial neocortical isolation model of epileptogenesis, prolonged hyperpolarization in non-traumatized neocortex near undercut leads to hyperexcitability and seizures. The long-term objective is to reduce these silent periods through exciting undamaged neurons neighboring the undercut. One means is using Gq-DREADD delivered to neurons via AAV viral vector. The preliminary results of experiment in our lab proved the effectiveness of this chemogenetic method. The main goal is to prevent posttraumatic epileptogenesis in human by determining the extent of excitability needed. Therefore, the use of cre-dependent transgenic mice is irrelevant in our study because it is different from posttraumatic conditions in which neurons are not genetically modified. Also using cre-lox system in humans could be challenging as it involves two types of recombination: intramolecular that is inversion or excision within the same DNA, and intermolecular which exchanges fragments between two DNA molecules (Lanza et al., 2012).

The main objective of this research project is to quantify the volume of neocortical transfection and the number of neurons transfected according to volume and titration of virus injected.

We hypothesize the neocortical transfection volume and the number of cells transfected depend on the volume and titration of virus injected. However, this relationship may not follow a linear pattern.

Chapter 2 Materials and Methods

All experiments were performed according to guidelines of Canadian Council on Animal Care and the protocol approved by the ethic committee of Université Laval. Adult male C57BL/6 mice were used in experiments. All mice had ad libitum access to food and water and were housed within individual cages in animal facility with a 12 h light/dark cycle.

2.1. Anesthesia in mice

Buprenorphine 0.3 mg/ml was injected (0.05-0.75 mg/kg) subcutaneously about 20 minutes before induction of anesthesia (according to Direction des Services Vétérinaires of Université Laval requirements).

The mice were anesthetized with Isoflurane (1-2%): 1-2L/min at induction, 0.6L/min for maintenance. Bupivacaine 2%/Lidocaine 0.5% was injected subcutaneously 0.05-0.07 ml/g around incision points. Incision started when pinch withdrawal reflex was absent. From the beginning of anesthesia until 48h after surgery, heating pads at 37°C were used to avoid hypothermia. Lactated Ringer solution (0.1ml/10g/h) was given subcutaneously at the beginning of anesthesia and hourly.

2.2. Surgical procedure

A midline incision of about 1 cm was performed and the galea was separated from underlying skull with a cotton-tip. Then two bur holes were made with microdrills on the left side: The first one at the junction between posterior border of coronal suture and medial border of sagittal suture (AP: -0.5mm; ML:0.5mm from bregma). The second hole was at 2mm behind the first one with coordinates AP:-2.5mm; ML:2mm from bregma. Pipettes were pulled from one mm OD borosilicate glass, with tip truncated to 10um diameter, and the tip was filled with aliquot containing AAV. The pipette lumen was previously irrigated with mineral oil and connected to nanoinjector (Nanoject-II), the automated device for injection of pre-set small liquid

volumes. The diapason of single shot injected volumes is between 2.3nl, and 69nl. Three different titrations of AAV2/8-hSyn-hM3D(Gq)-mCherry were used: 1.1E11gc/ml; 1.1E12gc/ml; 1.1E13gc/ml. In each animal only one of the titrations was used. We targeted layer V of neocortex at a depth of about 600um. After every single injection, the pipette remained for 5 minutes to avoid backflow through pipette track.

2.3. Brain sectioning

The mice were sacrificed 3 weeks after viral injection. The animals were deeply anesthetized with Ketamine/Xylazine and were perfused via transcardiac route initially with cold saline to wash out blood, and then by 4% paraformaldehyde (PFA). Then the brain was extracted from cranium and maintained in 4% PFA at 4°C in fridge for up to 48h. Caution was paid to avoid light exposure to brain from its extraction on. Aluminum foil was used to protect containers from light. The brain was sectioned into 50µm serial slices using vibrotome and then the sections were placed on microscope slides that were coverslipped the same day.

2.4. Image acquisition

Tissuescope 4000 slide scanner was used for image acquisition (Huron software). The serial images showing fluorescence were used to estimate transfection volume in a 3D-reconstructed image (Neurolucida 9 software) (figures 3C and 4C), and to automatically estimate transfected cells number (Image Pro 10 software) (figures 1D, 2C, and 4F). Image Pro parameters: Cellular diameter: 10-50 um, cellular roundness: 1-2, integrated Optical Density red: -1E+308 to 1E+308, region saturation: -1E+308 to 1E+306. The last two parameters were modified according to each image contrast and brightness.

Chapter 3 Results

We designed experiments for studying the effect of volume and titration of AAV vector injected, on cortical tissue transfection volume and number of cell transduction. We performed experiments using three different titrations and different volumes of AAV and then compared the results.

To analyze the data, in addition to raw data, we used corrected values to have normalized data. We also computed the relation between volumes of transfection and the number of cells transfected.

3.1. AAV 2/8 with titration 1.1E11 gc/ml could not transfect cortical regions or transduce neurons

A total of 12 injections were performed with 1.1E11 gc/ml titration. The volumes of virus-containing solution injected were as follows: 2.3 nl: 2 injections; 4.6 nl: 2 injections; 13.8 nl: 1 injection; 18.4 nl: 1 injection; 23 nl: 3 injections; 46 nl: 1 injection; 69 nl: 2 injections. With 1.1E11 gc/ml titration we did not find any neuron containing expected reporter.

It seems that the number of gene copies of this titration was not sufficient to transduce cells. Considering that in each nanoliter of this titration, there are 1.1E5 gene copies, and that in our results the lowest volumes of E12 and E13 capable of achieving transduction were 13.8 nl (15.18E6 gene copies) and 9.2 nl (10.12E7 gene copies), even 69 nl of 1.1E11 gc/ml titration delivers only 75.9E5 gene copies which is far behind those of higher titrations.

3.2. Experiment with AAV 2/8, titration 1.1E12 gc/ml intracortical injection

A total of six injections were performed with 1.1E12 gc/ml titration: 2.3 nl: 1 injection; 4.6 nl: 1 injection; 13.8 nl: 1 injection; 23 nl: 1 injection; 46 nl: 1 injection; 69 nl: 1 injection. The weak transfection of cortical tissue after injection of 13.8nl of AAV 2/8, titration 1.1E12 on the right hemisphere is shown in figure 1A. This transfected area is limited just like the number of neurons transduced in panels C and D which, respectively, show cells before and after automatic count with Image Pro. A stronger transfection with injection of 69nl of the same titration of AAV 2/8 was achieved as shown in figure 2A. The number of cells transfected was 1778. As

seen in panel D the magnified field was hypercellular which is in contrast with the pauci-cellularity in figure 1D.

No transduction was seen when 2.3 nl and 4.6 nl of AAV 2/8 were injected. The neocortical transfection volume and neuronal transduction number are summarized in figure 1E and 3D, respectively. With E12 titration, as the injection volume of AAV2/8 increases, more cells are transduced (figure 1E) and a larger transfection volume is observed (figure 3D). Pearson's correlation value of 0.97 (not shown) was calculated between AAV injection volume and the number of cells transduced (figure5, red curve), which confirms a robust linear correlation between these two parameters.

We expected transfection of a wide region of cortex and a larger number of neurons, as by increasing the volume of virus injected. The 1.1E12gc/ml follows this pattern in our experiment. Figure 7, red curve shows a nearly linear relation between AAV volume and the cortical transfection volume, and a Pearson's correlation value of 0.96 was calculated between these two parameters which means a strong correlation.

3.3. Experiment with AAV 2/8, titration 1.1E13 gc/ml intracortical injection

A total of eight injections were done with the 1.1E13 gc/ml titration: 2.3 nl: 1 injection; 4.6 nl: 2 injections; 9.2 nl: 1 injection; 18.4 nl: 1 injection; 23 nl: 1 injection; 46 nl: 1 injection; 55.2 nl: 1 injection. Figure 5 blue curve shows the correlation between AAV volume and number of neuronal transductions which is not totally linear except in its mid part. Pearson's correlation for these two parameters is 0.82, that means a strong enough correlation.

Neither of 2.3 nl or 4.6 nl volumes induced transfection. Yet, this is not clear why lower volumes of E13 could not transfect cells either. Therefore, there must be a lower level of volume in each titration, below which no transduction happens. It might be called the threshold transduction volume for each titration. It seems these volumes are too small to allow delivery of virus to cells. Cortical transfection volume with this titration was, as seen in figure 7 blue curve, not dependent in increase of AAV volume. It could increase or decrease with increases in AAV injection volume.

Pearson's correlation between AAV volume and cortical transfection volume was calculated -0.49 which means a weak correlation.

3.4. Corrected values of cell transduction in different titrations

In order to compare data obtained from one titration, and also to compare those values between different titrations, we calculated the expected cell transduction number for each 10 nl of AAV injected. For example, if injecting 13.8nl of E12 titration transduces 56 cells, injection of 10nl of the same titration might transduce 40.579 cells. Thus, the corrected cell counts for each 10 nl of E12 titration is as follows: 13.8nl: 40.6; 23nl: 64; 46nl: 147; 69 nl: 258 (127.4±98.34) (figure 7A red). Therefore, we conclude that higher volumes of injected virus with the titration E12 not only transfected globally more cells, but also transfected more cells per each 10 nl of injected virus.

The corrected value of cell counts for each 10 nl of E13 titration are the followings: 9.2 nl: 1028; 18.4 nl: 677; 23 nl: 543.50; 46 nl: 270; 55.2 nl: 354 (574.4± 299.37) (figure 7A blue). Thus, as mean, injection with E13 titration transfected roughly 5 times more cells than injections with E12 titration. However, the number of transfected cells with higher virus concentration in injected solution (E13), did not depend on the volume of injected solution. It was likely some kind of saturation, in which a small injected volume already transfected majority of cells that could be targeted by this virus.

Comparing these two titrations, t-score was 3.1341, and p-value was 0.0034 which means a significant difference between these two titrations in transducing cells.

The corrected values for cortical transfection volume (um^3) per 10 nl AAV injected with titration E12 are the followings: 13.8nl: 61106; 23nl: 189460; 46nl: 195401; 69 nl: 158875 (151210±62165) (figure 7B red). Therefore, despite a steady increase in transfection volume relating to increased AAV volume, the corrected values for E12 does not respect this rule at highest AAV injected volume (69 nl). The corrected values for transfection volume in um^3 for each 10 nl of AAV injected, titration E13 are as follows: 9.2 nl: 9655565; 18.4 nl: 792516; 23 nl: 105673; 46 nl:

301670; 55.2 nl: 401402 (2251365±4146628) (figure 7B blue). So, the mean corrected transfection volume per 10 nl AAV is about 15-fold with E13 titration as compared to E12 titration. The t-test is -1.1323 and p-value= 0.8396. Therefore, the different transfection volumes obtained with each 10nl AAV injection with either E12 or E13 titrations are not statistically meaningful.

3.5. Relation between transfection volume and number of cells transduced

Next, we computed the relation between volume of tissue affected by viral injection and the number of transfected cells. Pearson's correlation was 0.88101 for E12, and -0.43648 for E13 titrations. That means there is a positive correlation between tissue volume transfection and neuronal transduction with E12 titration, whereas with E13 titration the correlation between these two parameters was weak (figure 4G).

Chapter 4 Discussion

In this study we investigated the effect of AAV titration and its volume of injection on the volume of cortical transfection and the number of cells transduced. This may ultimately guide us in choosing the right titration and injection volume of AAV in order to alter epileptogenesis.

Two common features of all kinds of epilepsies are: 1) unprovoked seizures 2) the abnormal local neuronal synchronization (Timofeev et al., 2013). The main neuronal activity change that was observed during epileptogenesis is increased neuronal silence, which as consequence, up-regulates neuronal and network excitability that leads to seizure generation (Topolnik et al., 2003a; Timofeev, 2005; Timofeev, 2011). Therefore, it seems that an increase in local excitability of traumatized cortex immediately after trauma should shorten neuronal silence and thus prevent epileptogenesis. This might be achieved with low-intensity electrical stimulation or pharmacologically using drugs that affect K^+, Na^+, or Ca^{2+} homeostasis) (Topolnik et al., 2003a; Houweling et al., 2005; Timofeev, 2011).

Indeed, preliminary data obtained in our lab show that moderate increase in excitability around the undercut cortex prevented epileptogenesis, but major increase in excitability was epileptogenic by itself. Because in previous experiments carried out in our lab, the AAV serotype 2/8 was used to counter epileptogenesis, we used the same serotype as well. We tested 3 titrations and different volumes of the same AAV 2/8 carrying Gq-DREADD. With E11 titration, no neuronal transduction was achieved. This might be because this low concentration does not deliver enough gene copies to neurons, or due to the phagocytosis by astrocytes and microglia of virus and genes it carries. Because this experiment was performed for the first time, the lack of comparison with other studies reduces its reliability. A somewhat similar experiment has been performed by Dayton and coworkers (Dayton et al., 2018). They tested three different doses of AAV PHP EB, as they called low dose (1.2E13 vector genome/kg), mid-dose (3.6E13 vg/kg), and high dose (1.2E14 vg/kg). Each dose was injected to three adult rats. They observed a consistent dose dependent GFP expression in rat cerebellum ($p<0.05$). They also noticed a brighter fluorescence with mid-dose. Our AAV dose was much lower, and injections were

performed in the mouse neocortex, not in the cerebellum. This might explain the difference in results obtained.

In our experiments, it seems that E11 titration was too low to transduce neurons. In our series, low volumes of AAV injections, that is 2.3 nl and 4.6 nl were not able to transduce cells. This might be due to rapid clearance of these aqueous solutions by extracellular environment although we cannot exclude the possibility that with such small volumes the used nanoinjector was unable to really release solution in extracellular space. When comparing E12 and E13 titrations in terms of absolute values of neuronal transduction, the E12 showed strong positive correlation with AAV volume injected ($r = 0.97$), whereas Pearson's correlation for E13 was 0.82. The corrected values of transduction number for each 10 nl of AAV injected indicated values range of 127.4±98 cells for E12, and 574.4±299 for E13. The t-value is -3.1341. The p-value is 0.0034, so there is a significant difference between using E12 vs. E13 for cell transduction. For the corrected values of cortical transfection volume for each 10 nl of AAV injection, range of values was 151210.5±62165 μm^3 in E12, and 2251365±4146628 μm^3 for E13. The t-value is -1.1323, and the p-value is 0.8396. Therefore, using either E12 or E13 for transfecting the cortex yield no statistically significant results. With regard to these two results, the transfection volume for each 10 nl of E13 is in average 15 times more than that of E12 titration, while the neuronal transduction number for each 10 nl of E13 is about 5 times that of E12 titration. It might indicate a more widespread expression of viral genes in each neuron with E13 as compared with E12 titration. The functional unit in central nervous system is the neuron, but whether a more saturated viral spread or a confined one would act better for getting an antiepileptogenic effect needs to be determined by further investigation.

Potential pitfalls

Despite the care taken for conducting a well-performed study, there could have been some issues affecting the final results. The age of animals may affect the cell transduction. The pipette might have been blocked, or even leaking, delivering AAV below or over the set volume. Using the same pipette to inject two different locations

could break the tip or the shaft of pipette and deliver an out-of-control AAV volume. The shrinkage and desiccation of brain section during cutting, spreading, or coverslipping may have an effect on fluorescence detected. Image acquisition with slide scanner can be tricky. Images on the same slide could have different levels of brightness and contrast. Sometimes red laser doesn't work properly. That can lead to a lack of fluorescence detection despite its expected presence. In acquired images, changing the brightness and the contrast can affect interpretation of dots and particles seen, and can be misleading in differentiating neurons from image artifacts. When estimating transfection volume, it is challenging to define the limits of transfection if there is no visible border and staining, especially with dispersed transduced cells. The fluorescent particles may show a variety of shapes, making neurons and artifacts hardly distinguishable or even indistinguishable.

Another problem encountered was the covid-19 pandemic and multiple lab closures. We lost some of our ongoing experiments. The number of experiments for this study was reduced as a result of shortage of time.

Conclusion

Our results show a more reliable and predictable neuronal transduction with E12 titration. Even if the sample size is not big enough, the high positive correlation and almost linear distribution of transduction by E12 titration is promising. Although E13 titration may also be used for transducing neurons, the non-linear distribution in our study puts its reliability in doubt. Further studies with both E12 and E13 titrations should be done in order to confirm our results. It seems that E11 titration is not capable of transducing cells and should no longer be used in our future experiments.

The next step would be the quantification of transduction in traumatized cortex, which might have different extent and investigating the antiepileptogenic effect in relation to number of transduced cells.

For the purpose of presentation, some brain images were edited only after automatic cell count was performed. These retouches were not done in or near the injection site where the fluorescence was visible. So, these modifications did not change the results of research in any way.

Figures

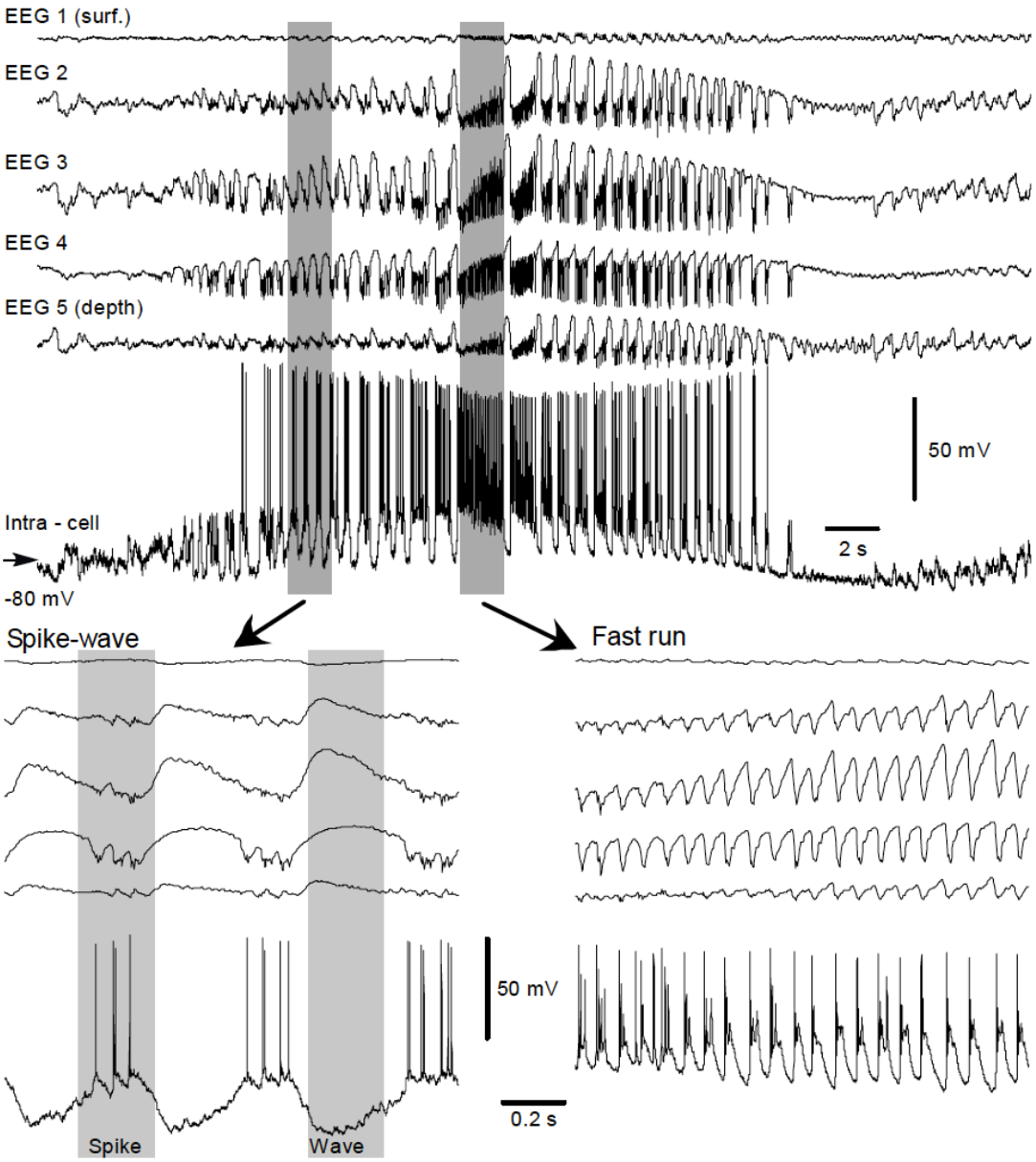

Figure I-1. Idiopathic electrographic seizure recorded from cortical area 5 of cat anesthesized with ketamine-xylazine. Five upper traces show local field potentials recorded from cortical surface and different depth. The lower trace shows an intracellular recording of a cortical neuron during spiking activity. The lowermost traces are selected time period of the same neuron during its spike-wave alterations and fast runs (Timofeev and Bazhenov, 2005).

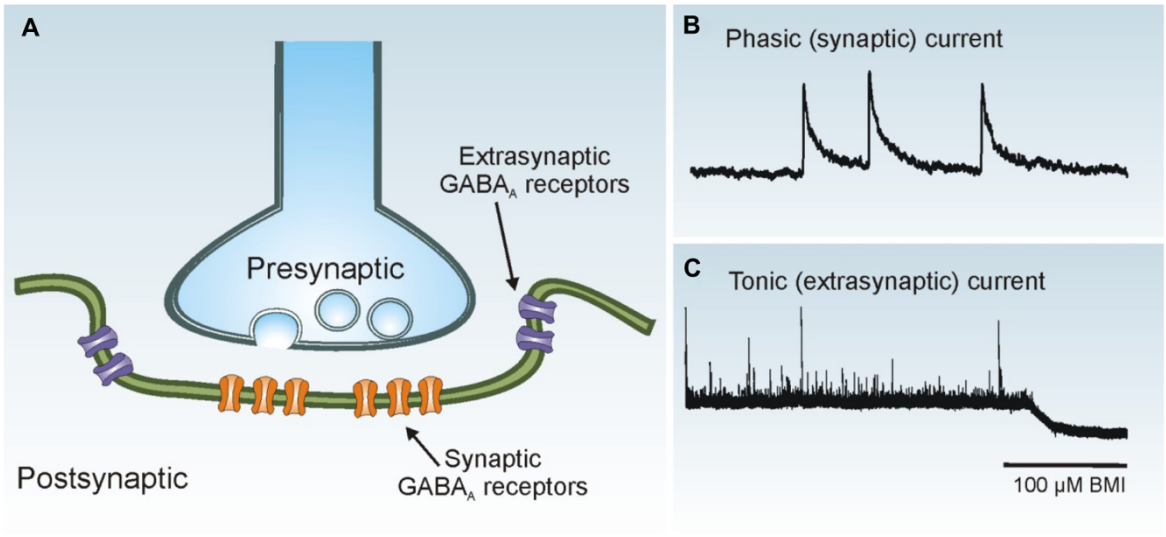

Figure I-2. Phasic and tonic GABAA receptor activation. **A.** Synaptic receptors (orange) are located on the postsynaptic membrane just beneath presynaptic release sites,whereas extrasynaptic receptors (purple) are located away from the synaptic junction. **B.** Phasic (synaptic) IPSCs are rapid events. Three individual IPSCs are shown in a whole-cell voltage-clamp recording obtained from a dentate granule cell. **C.** The tonic (extrasynaptic) current in this granule cellis revealed as a baseline shift after application of the $GABA_A$ receptor antagonist bicuculline methiodide (BMI;100 µM) (Hunt et al., 2013).

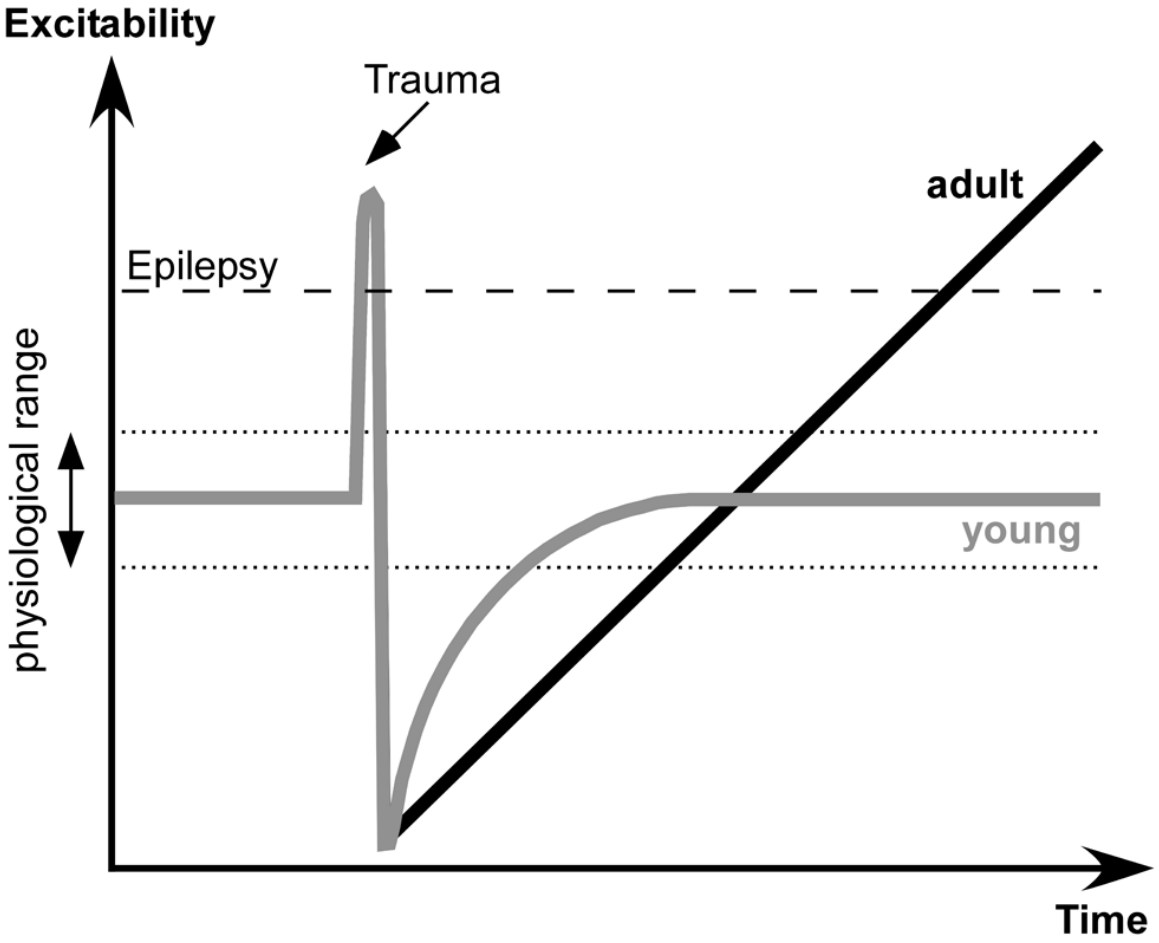

Figure I-3. Proposed dynamics of network excitability induced by brain trauma in young and adult subjects. After initial insult, there is a brief period of hyperexcitability. Then the neuronal activity in injured area is diminished dramatically. 2-4 Weeks after trauma, the excitability reaches the baseline level. While in adults in may progress to epilepsy, in young animals it usually remains in steady state (Timofeev et al., 2013).

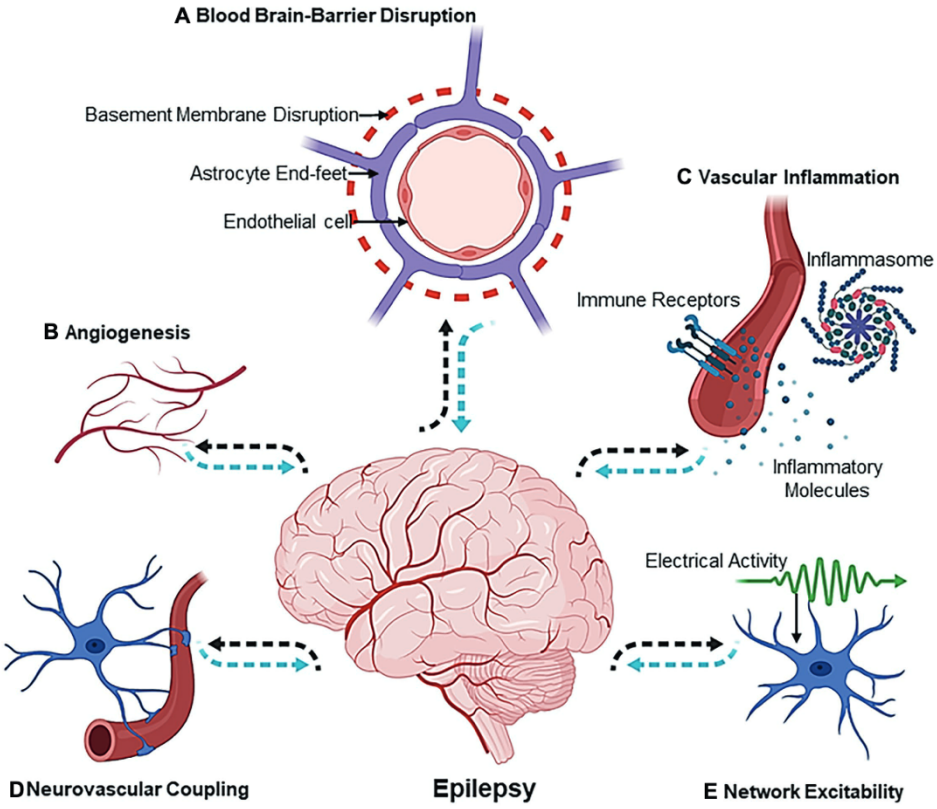

Figure I-4. The Vascular Landscape in Epilepsy. The mechanisms involved in the etiology of epileptogenesis are multiphasic [**A**. blood-brain-barrier disruption, **B.** angiogenesis, **C**. vascular inflammation, **D**. neurovascular coupling and, lastly, **E**. network excitability] and exist at the crossroads of the neurovascular network. Dotted black arrows indicate the sequence of events leading up to epileptogenesis, whereas dotted blue arrows show the sequence of events that affect the neuron or vascular interface in an epileptic brain. Illustration was created using Biorender.com (Baruah et al., 2019).

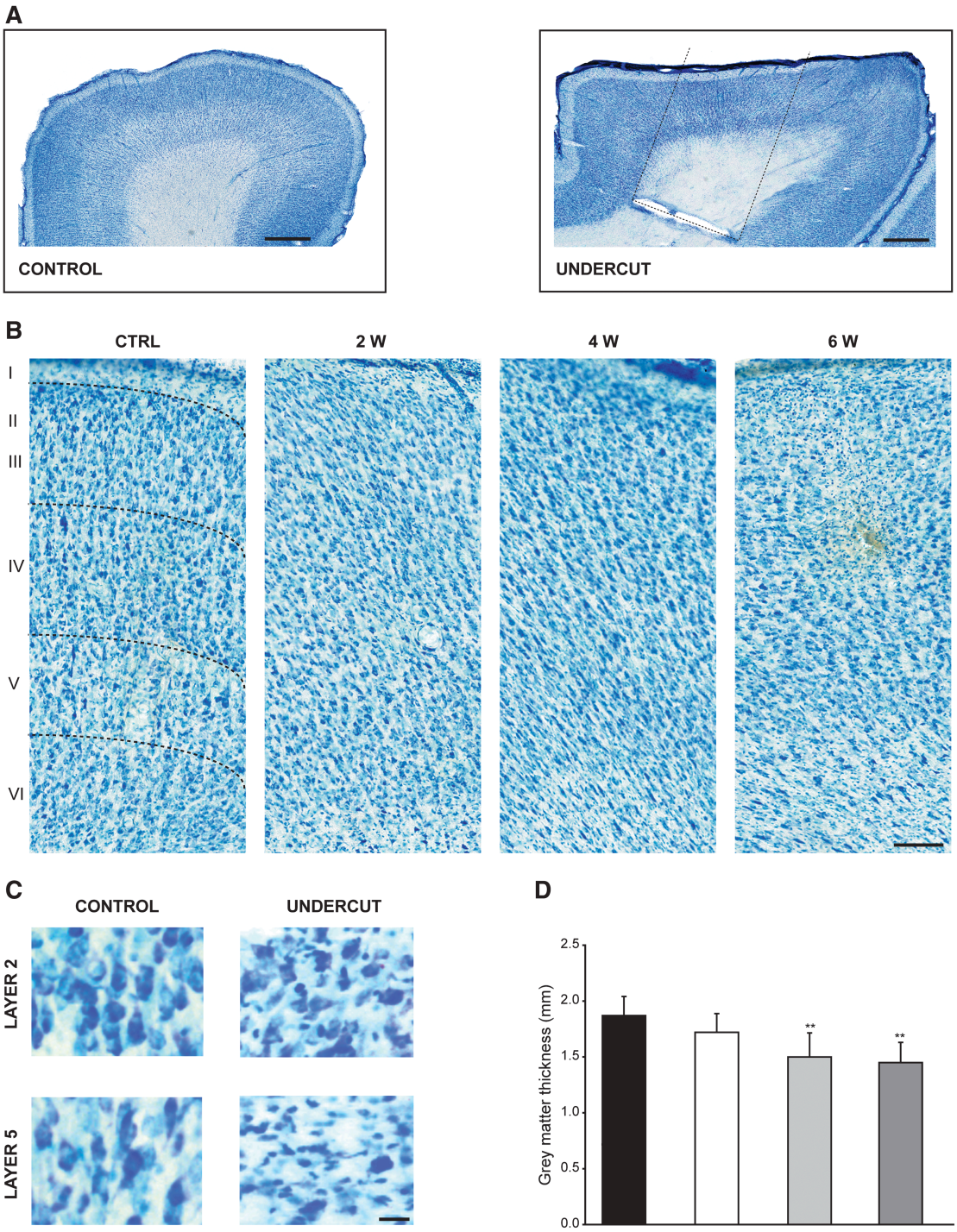

Figure I-5. Neocortical Post-Traumatic Epileptogenesis Is Associated with Loss of GABAergic Neurons. **A**. Reduced cortical thickness in undercut. **B**. Changes in six cortical layers 2-, 4-, and 6-weeks following trauma as compared with the normal structure (CTRL). **C**. neuron loss is more prominent in layer 5 than layer 2. **D.** Loss of gray matter thickness with times mentioned in panel B (Avramescu et al., 2009).

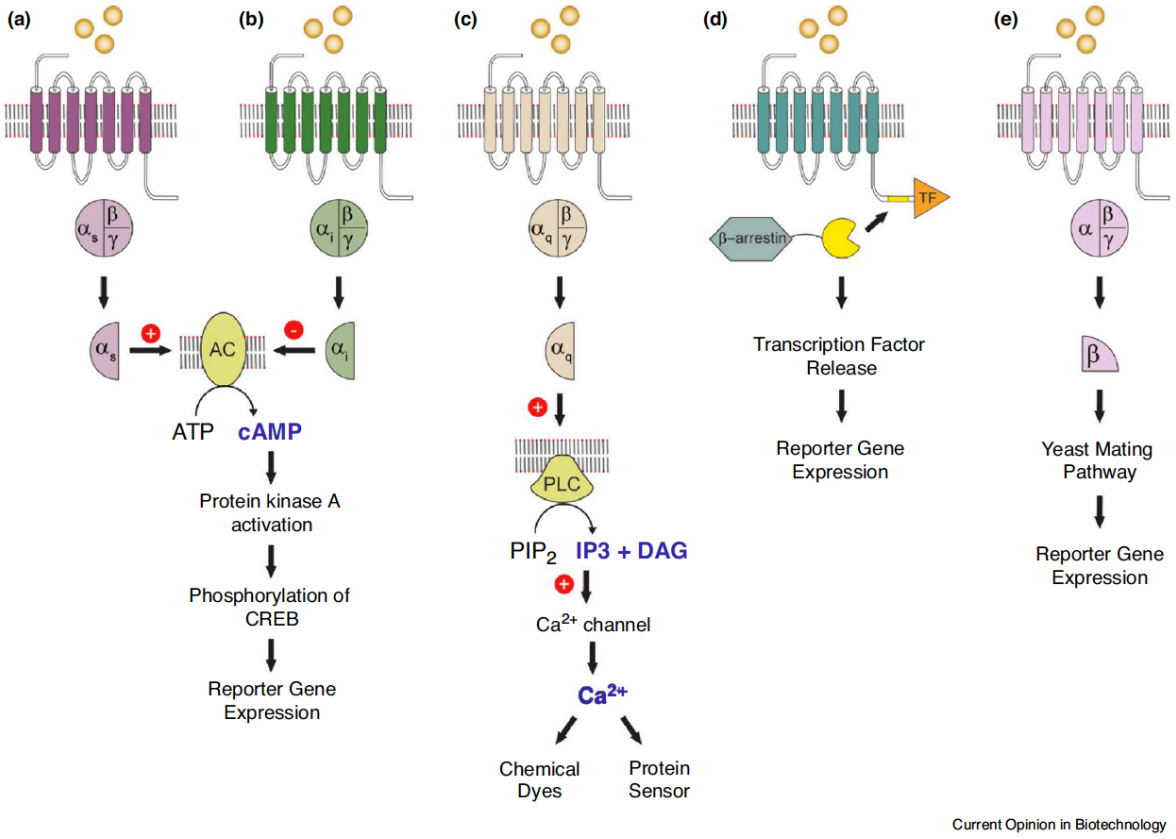

Figure I-6. High-throughput GPCR cell-based assays. (**a**) GPCR activation of Gas upregulates adenylate cyclase (AC) resulting in increased cAMP levels. cAMP activates protein kinase A, which phosphorylates the transcription factor CREB ultimately resulting in reporter gene expression. (**b**) GPCR activation of Gai downregulates AC resulting in a decrease of cAMP levels. (**c**) GPCR activation of Gaq upregulates phospholipase C (PLC), which breaks down PIP2 (phosphatidylinositol biphosphate) into IP3 (inositol triphosphate) and DAG (diacylglycerol). IP3 goes on to activate Ca2+ channels in the endoplasmic reticulum increasing the Ca2+ concentration in the cytosol, which is detected via chemical dyes or protein sensors. (**d**) In b-arrestin recruitment-based assays, GPCR activation recruits b-arrestin linked to a protease (yellow) that cleaves the transcription factor (TF) linked to the GPCR via a protease cleavable linker (yellow). Transcription factor release ultimately results in reporter gene expression. (**e**) In Saccharomyces cerevisiae, human GPCRs can couple to yeast or human/yeast Ga chimeras and via Gb activate the yeast mating pathway ultimately leading to expression of a reporter gene. Gold circles: agonist (Yasi et al., 2020).

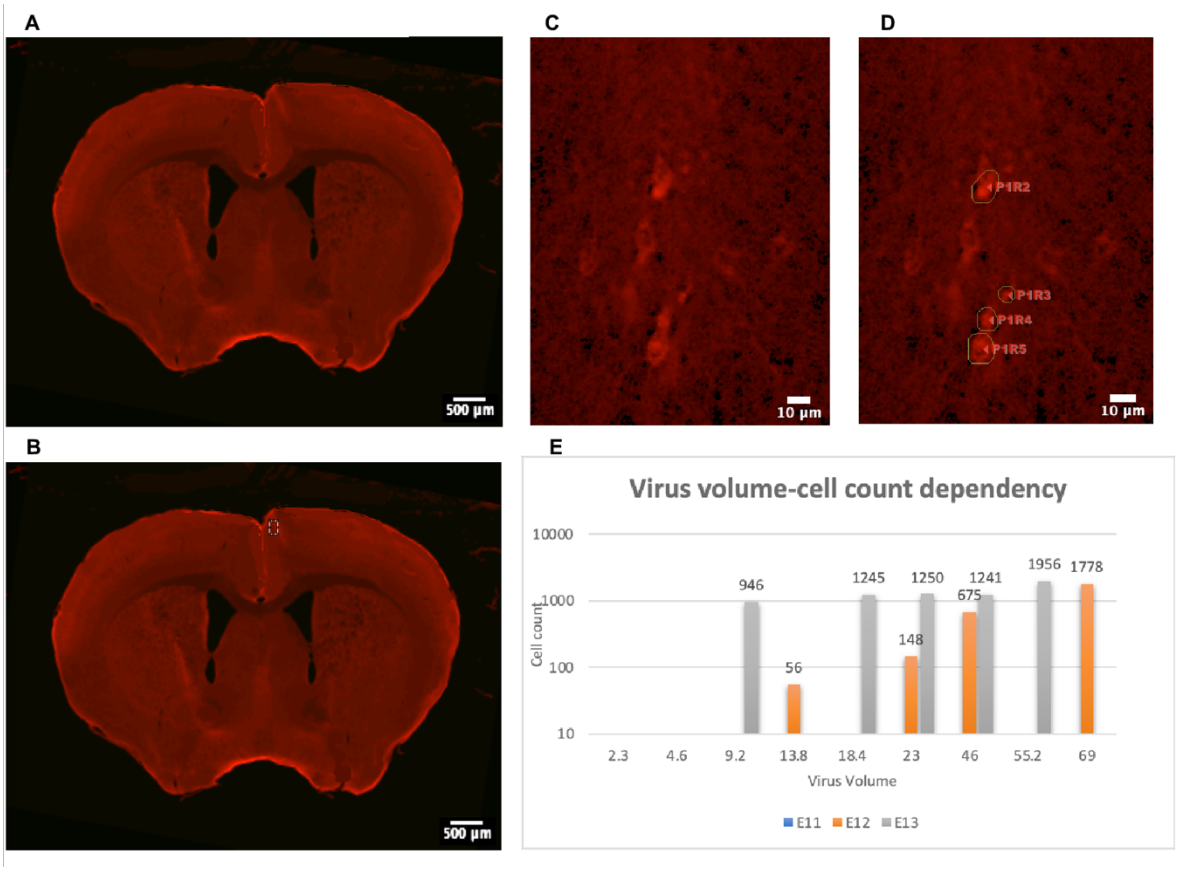

Figure 1- Transfection detected 3 weeks after injection of 13.8 nl, titration 1.1E12 gc/ml of AAV2/8-hSyn-hM3D(Gq)-mCherry in a 50µm brain section. **A**. Cortical transfection can be seen in right hemisphere near midline. **B.** The inlet defines the area selected for detecting cell transfection. **C.** Bright red fluorescence of mCherry in neurons. **D.** Automatic cell count with Image Pro software. In this panel four cells are detected. **E.** The graph shows number of transduced cells according to the volume of virus injected. The orange bars show E12 titration results, and the gray bars those of E13 titration. No transduction was found with E11 titration.

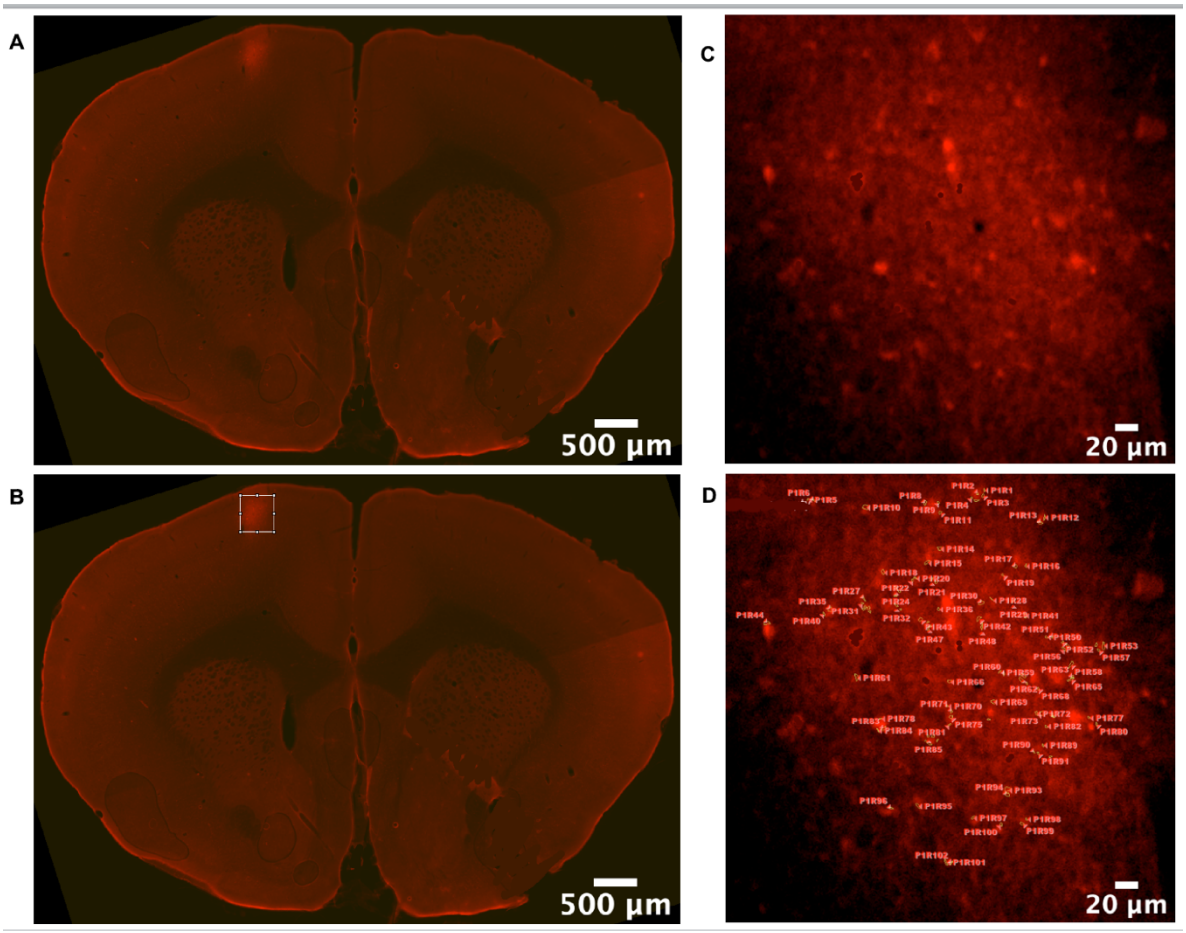

Figure 2– Transfection found 3 weeks after injecting 69nl of AAV2/8-hSyn-hM3D(Gq)-mCherry, titration 1.1E12gc/ml. **A.** Cortical transfection in a 50µm thick brain section is seen as a bright red spot on the left side at about 1000µm distance from midline. **B.** The square shows region of interest for detecting cells. This region in magnified in images C and D. **C.** Red dots indicate the fluorescence caused by mCherry in neurons. **D.** Neurons are detected automatically with Image Pro.

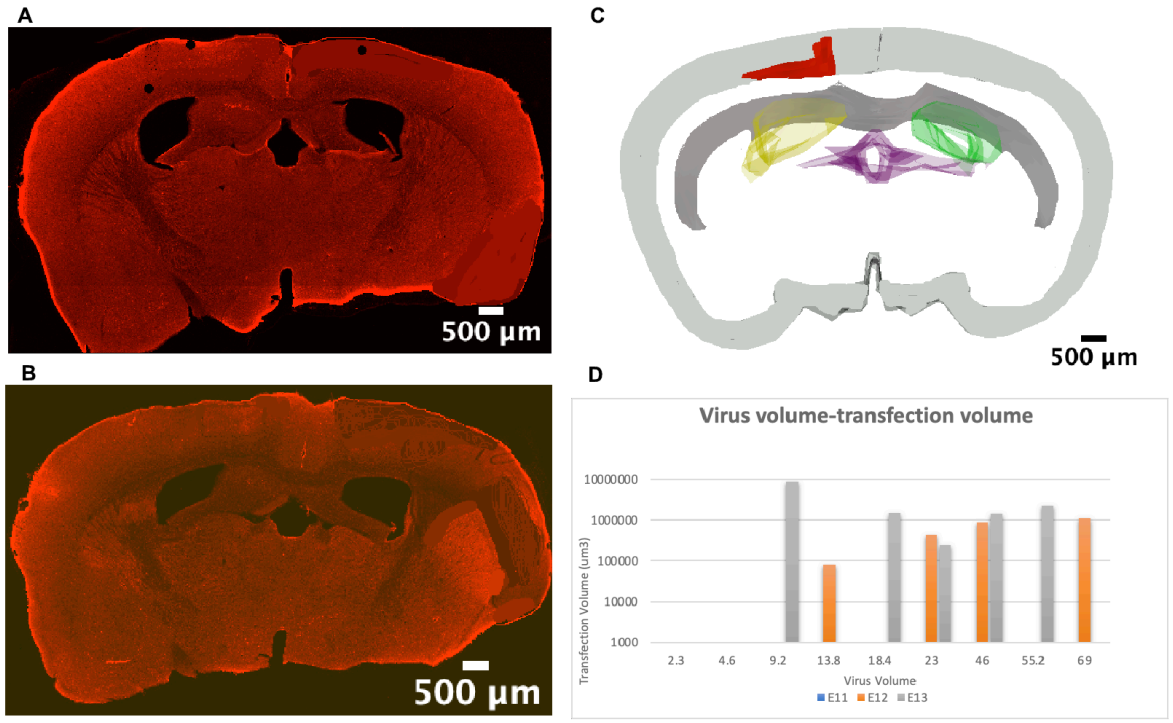

Figure 3- Cortical transfection after injection of 18.4 nl of AAV2/8-hSyn-hM3D(Gq)-mCherry, 1.1E13 titration. **A.** and **B.** 50µm brain section showing cortical transfection on the left side. **C.** 3D reconstruction of the same experiment with Neurolucida from 12 brain sections. Transfection volume was estimated about 1458230 μm^3 by the software. **D.** The graph shows the cortical volume transfection (μm^3) as logarithmic values in Y-axis achieved by different AAV injection volume (nl) in X-axis for E12 (orange bars) and E13 (gray bars) titrations. N.B. some imperfections in image B were retouched which were far from injection site.

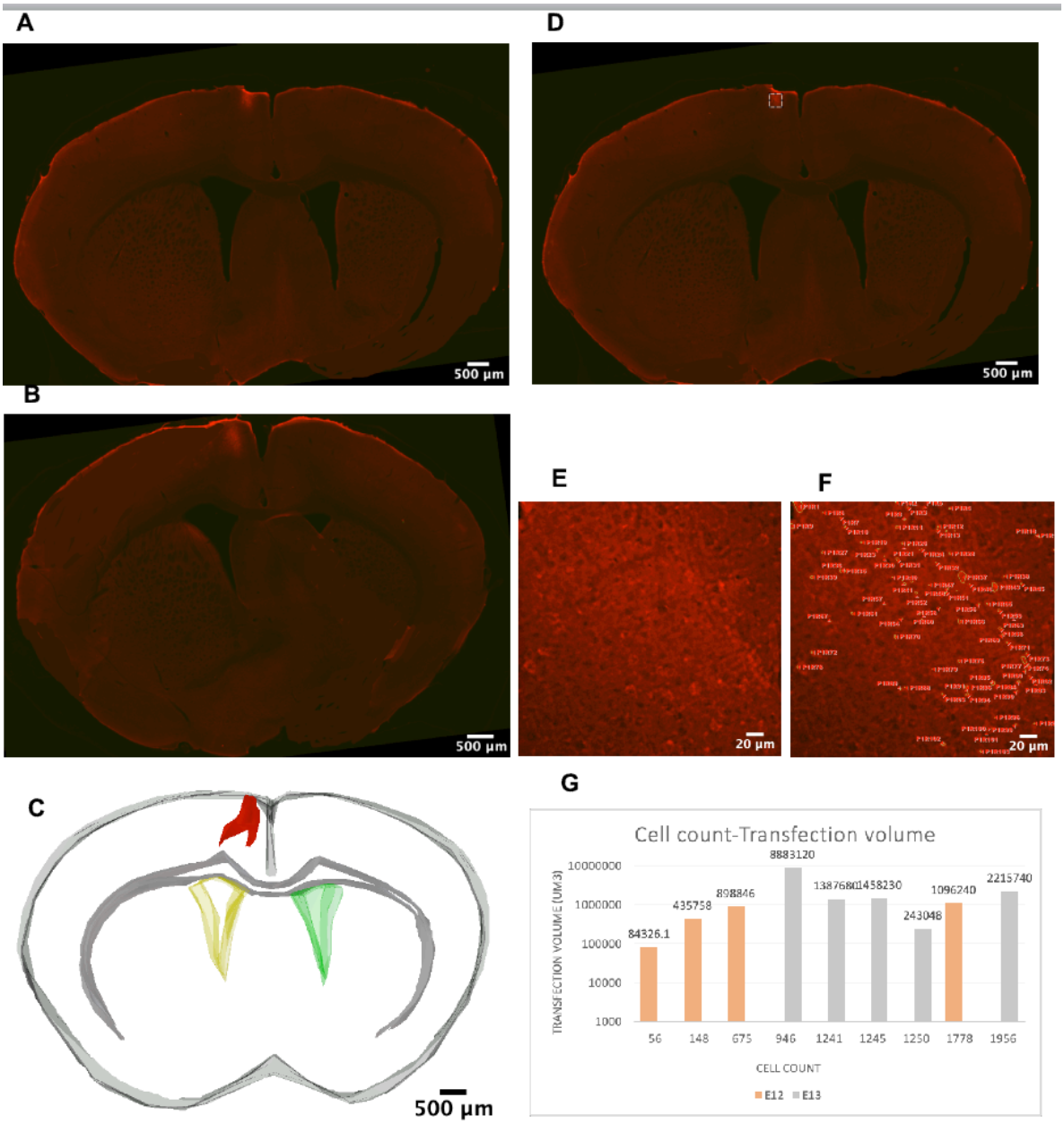

Figure 4- An example of cortical transfection and cell transduction detected 3 weeks after injecting 9.2 nl of AAV2/8-hSyn-hM3D(Gq)-mCherry,1.1E13 titration. **A.** and **B.** show two 50µm thick brain sections with transfected cortex on the left side of midlne. **C.** 3D reconstruction of ten 50µm sections using Neurolucida. The transfection volume was estimated 8883120µm^3 by the software. **D.** The square indicates the region of interest in the same section as panel A, for detecting cells. The magnified images of this inlet are seen in panels E and F. **E.** Fluorescence caused by mCherry is visible as bright red dots. **F.** Automatic detection of transduced neurons by Image Pro software. **G.** In this chart, the relation between the number of neurons transduced (X-axis) and the cortical transfection volume (in µm^3, logarithmic values in Y-axis) obtained with different AAV volumes and titrations (E12: orange; E13: gray) are shown. N.B. some retouch of image B far from injection site.

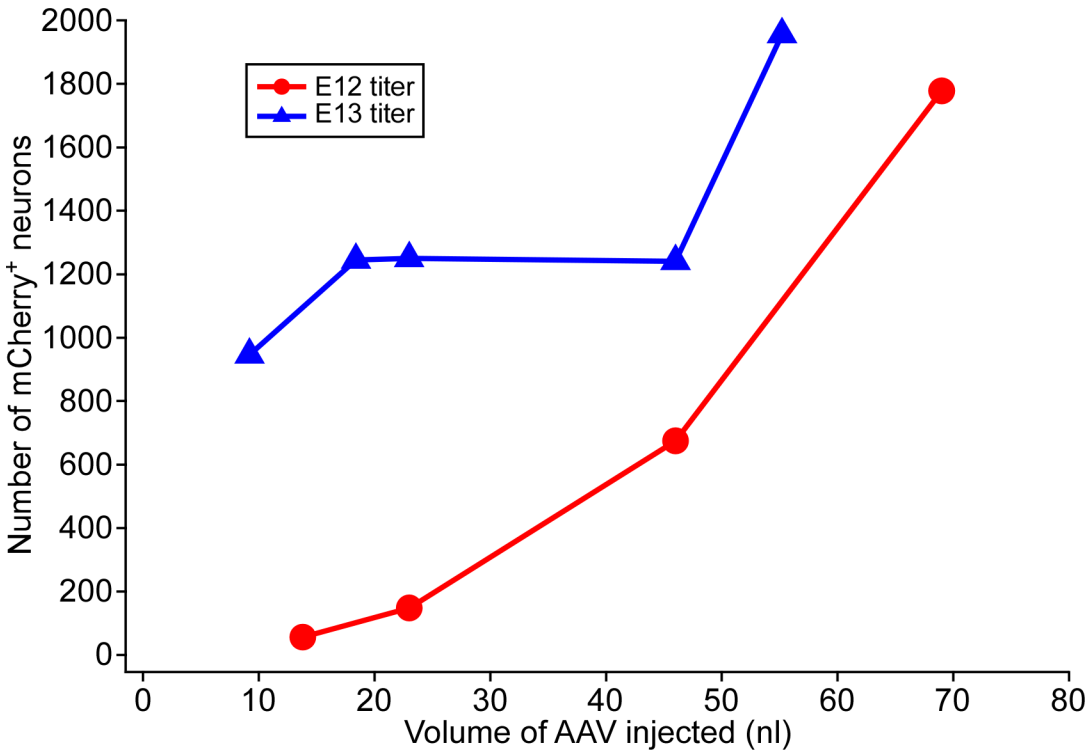

Figure 5- Correlation between injected AAV volume and cell transduction. With E12 titration (red) the correlation is quasi-linear but with E13 titration (blue) it is not.

.

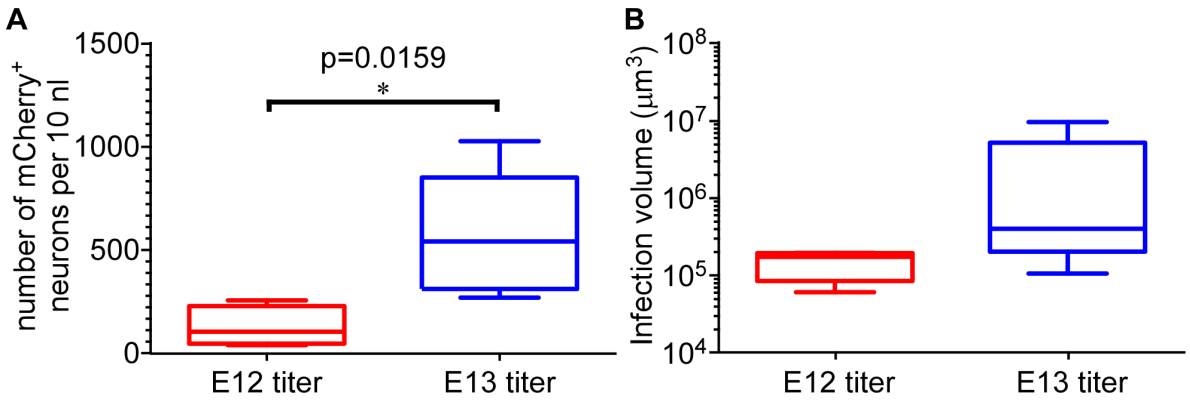

Figure 6- Corrected values for each 10 nl AAV injected, with E12 and E13 titrations. A. Boxplot comparison of corrected values of cell transduction. The mean value of corrected cell number with E13 is about 5-fold that of E12 titration. The t-value for cell transduction was -2.83471, and p-value 0.0159 that is significant. B. For volume transfection with these two titrations, t-value and p-value were -0.99869, and 0.351207 respectively which means no significant difference.

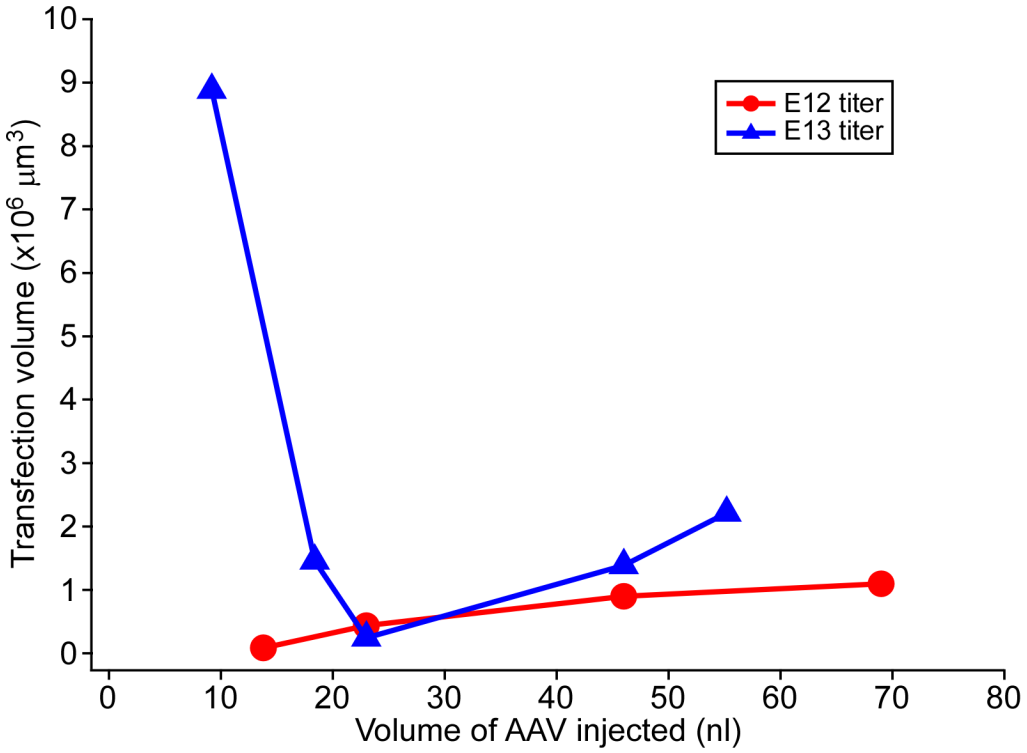

Figure 7- Correlation between volume (nl) of AAV injected and transfection volume (μm^3). Y-axis shows the transfection volume. With E12 (red) titration there is a linear correlation, but with E13 (blue) titration the correlation is curved.

Bibliography

Agbandje-McKenna M, Kleinschmidt J (2011) AAV capsid structure and cell interactions. Methods Mol Biol 807:47-92.

Ajmone-Marsan C, Ralston B (1956) Thalamic control of certain normal and abnormal cortical rhythms. Electroencephalogr Clin Neurophysiol 8:559-582.

Alexander GM, Rogan SC, Abbas AI, Armbruster BN, Pei Y, Allen JA, Nonneman RJ, Hartmann J, Moy SS, Nicolelis MA, McNamara JO, Roth BL (2009) Remote control of neuronal activity in transgenic mice expressing evolved G protein-coupled receptors. Neuron 63:27-39.

Armbruster BN, Li X, Pausch MH, Herlitze S, Roth BL (2007) Evolving the lock to fit the key to create a family of G protein-coupled receptors potently activated by an inert ligand. Proc Natl Acad Sci U S A 104:5163-5168.

Aronica E, Fluiter K, Iyer A, Zurolo E, Vreijling J, van Vliet EA, Baayen JC, Gorter JA (2010) Expression pattern of miR-146a, an inflammation-associated microRNA, in experimental and human temporal lobe epilepsy. Eur J Neurosci 31:1100-1107.

Avramescu S, Timofeev I (2008) Synaptic strength modulation after cortical trauma: a role in epileptogenesis. J Neurosci 28:6760-6772.

Avramescu S, Nita DA, Timofeev I (2009) Neocortical post-traumatic epileptogenesis is associated with loss of GABAergic neurons. J Neurotrauma 26:799-812.

Ayoub A, Aumann D, Horschelmann A, Kouchekmanesch A, Paul P, Born J, Marshall L (2013) Differential effects on fast and slow spindle activity, and the sleep slow oscillation in humans with carbamazepine and flunarizine to antagonize voltage-dependent Na+ and Ca2+ channel activity. Sleep 36:905-911.

Babb TL, Pretorius JK, Kupfer WR, Crandall PH (1989) Glutamate decarboxylase-immunoreactive neurons are preserved in human epileptic hippocampus. J Neurosci 9:2562-2574.

Babb TL, Kupfer WR, Pretorius JK, Crandall PH, Levesque MF (1991) Synaptic reorganization by mossy fibers in human epileptic fascia dentata. Neuroscience 42:351-363.

Bal T, von Krosigk M, McCormick DA (1995) Synaptic and membrane mechanisms underlying synchronized oscillations in the ferret lateral geniculate nucleus in vitro. J Physiol 483 (Pt 3):641-663.

Barkmeier DT, Loeb JA (2009) An animal model to study the clinical significance of interictal spiking. Clin EEG Neurosci 40:234-238.

Baruah J, Vasudevan A, Kohling R (2019) Vascular Integrity and Signaling Determining Brain Development, Network Excitability, and Epileptogenesis. Front Physiol 10:1583.

Bazhenov M, Timofeev I, Frohlich F, Sejnowski TJ (2008) Cellular and network mechanisms of electrographic seizures. Drug Discov Today Dis Models 5:45-57.

Beattie EC, Stellwagen D, Morishita W, Bresnahan JC, Ha BK, Von Zastrow M, Beattie MS, Malenka RC (2002) Control of synaptic strength by glial TNFalpha. Science 295:2282-2285.

Beaulieu C (1993) Numerical data on neocortical neurons in adult rat, with special reference to the GABA population. Brain Res 609:284-292.

Beaumont TL, Yao B, Shah A, Kapatos G, Loeb JA (2012) Layer-specific CREB target gene induction in human neocortical epilepsy. J Neurosci 32:14389-14401.

Beevers CS, Chen L, Liu L, Luo Y, Webster NJ, Huang S (2009) Curcumin disrupts the Mammalian target of rapamycin-raptor complex. Cancer Res 69:1000-1008.

Ben-Ari Y (1985) Limbic seizure and brain damage produced by kainic acid: mechanisms and relevance to human temporal lobe epilepsy. Neuroscience 14:375-403.

Berns KI, Linden RM (1995) The cryptic life style of adeno-associated virus. Bioessays 17:237-245.

Berns KI, Giraud C (1996) Biology of adeno-associated virus. Curr Top Microbiol Immunol 218:1-23.

Bertram EH, Cornett J (1993) The ontogeny of seizures in a rat model of limbic epilepsy: evidence for a kindling process in the development of chronic spontaneous seizures. Brain Res 625:295-300.

Bertram EH, Cornett JF (1994) The evolution of a rat model of chronic spontaneous limbic seizures. Brain Res 661:157-162.

Blander G, Guarente L (2004) The Sir2 family of protein deacetylases. Annu Rev Biochem 73:417-435.
Botta J, Appelhans J, McCormick PJ (2020) Continuing challenges in targeting oligomeric GPCR-based drugs. Prog Mol Biol Transl Sci 169:213-245.
Bouyer JJ, Tilquin C, Rougeul A (1983) Thalamic rhythms in cat during quiet wakefulness and immobility. Electroencephalogr Clin Neurophysiol 55:180-187.
Brailowsky S, Menini C, Silva-Barrat C, Naquet R (1987) Epileptogenic gamma-aminobutyric acid-withdrawal syndrome after chronic, intracortical infusion in baboons. Neurosci Lett 74:75-80.
Brailowsky S, Kunimoto M, Silva-Barrat C, Menini C, Naquet R (1990) Electroencephalographic study of the GABA-withdrawal syndrome in rats. Epilepsia 31:369-377.
Brennan GP, Dey D, Chen Y, Patterson KP, Magnetta EJ, Hall AM, Dube CM, Mei YT, Baram TZ (2016) Dual and Opposing Roles of MicroRNA-124 in Epilepsy Are Mediated through Inflammatory and NRSF-Dependent Gene Networks. Cell Rep 14:2402-2412.
Buckmaster PS (2012) Mossy Fiber Sprouting in the Dentate Gyrus. In: Jasper's Basic Mechanisms of the Epilepsies (th, Noebels JL, Avoli M, Rogawski MA, Olsen RW, Delgado-Escueta AV, eds). Bethesda (MD).
Buckmaster PS, Dudek FE (1997) Network properties of the dentate gyrus in epileptic rats with hilar neuron loss and granule cell axon reorganization. J Neurophysiol 77:2685-2696.
Buckmaster PS, Zhang GF, Yamawaki R (2002) Axon sprouting in a model of temporal lobe epilepsy creates a predominantly excitatory feedback circuit. J Neurosci 22:6650-6658.
Calixto E, Lopez-Colome AM, Casasola C, Montiel T, Bargas J, Brailowsky S (2000) Neocortical hyperexcitability after GABA withdrawal in vitro. Epilepsy Res 39:13-26.
Canto C, Auwerx J (2012) Targeting sirtuin 1 to improve metabolism: all you need is NAD(+)? Pharmacol Rev 64:166-187.
Castle MJ, Turunen HT, Vandenberghe LH, Wolfe JH (2016) Controlling AAV Tropism in the Nervous System with Natural and Engineered Capsids. Methods Mol Biol 1382:133-149.
Castro-Alamancos MA (1999) Neocortical synchronized oscillations induced by thalamic disinhibition in vivo. J Neurosci 19:RC27.
Cauli B, Audinat E, Lambolez B, Angulo MC, Ropert N, Tsuzuki K, Hestrin S, Rossier J (1997) Molecular and physiological diversity of cortical nonpyramidal cells. J Neurosci 17:3894-3906.
Chang SE, Todd TP, Bucci DJ, Smith KS (2015) Chemogenetic manipulation of ventral pallidal neurons impairs acquisition of sign-tracking in rats. Eur J Neurosci 42:3105-3116.
Chen Y, Xie Y, Wang H, Chen Y (2013) [SIRT1 expression and activity are up-regulated in the brain tissue of epileptic patients and rat models]. Nan Fang Yi Ke Da Xue Xue Bao 33:528-532.
Chu K, Jung KH, Lee ST, Kim JH, Kang KM, Kim HK, Lim JS, Park HK, Kim M, Lee SK, Roh JK (2008) Erythropoietin reduces epileptogenic processes following status epilepticus. Epilepsia 49:1723-1732.
Cohen I, Navarro V, Clemenceau S, Baulac M, Miles R (2002) On the origin of interictal activity in human temporal lobe epilepsy in vitro. Science 298:1418-1421.
Compston A (2010) The Berger rhythm: potential changes from the occipital lobes in man. Brain 133:3-6.
Cowan RL, Wilson CJ (1994) Spontaneous firing patterns and axonal projections of single corticostriatal neurons in the rat medial agranular cortex. J Neurophysiol 71:17-32.
Cronin J, Dudek FE (1988) Chronic seizures and collateral sprouting of dentate mossy fibers after kainic acid treatment in rats. Brain Res 474:181-184.
Cronin J, Obenaus A, Houser CR, Dudek FE (1992) Electrophysiology of dentate granule cells after kainate-induced synaptic reorganization of the mossy fibers. Brain Res 573:305-310.
Danober L, Deransart C, Depaulis A, Vergnes M, Marescaux C (1998) Pathophysiological mechanisms of genetic absence epilepsy in the rat. Prog Neurobiol 55:27-57.
Dayton RD, Grames MS, Klein RL (2018) More expansive gene transfer to the rat CNS: AAV PHP.EB vector dose-response and comparison to AAV PHP.B. Gene Ther 25:392-400.
DeFazio RA, Keros S, Quick MW, Hablitz JJ (2000) Potassium-coupled chloride cotransport controls intracellular chloride in rat neocortical pyramidal neurons. J Neurosci 20:8069-8076.

DeFelipe J (1997) Types of neurons, synaptic connections and chemical characteristics of cells immunoreactive for calbindin-D28K, parvalbumin and calretinin in the neocortex. J Chem Neuroanat 14:1-19.
DeFelipe J, Farinas I (1992) The pyramidal neuron of the cerebral cortex: morphological and chemical characteristics of the synaptic inputs. Prog Neurobiol 39:563-607.
Desai NS, Rutherford LC, Turrigiano GG (1999) Plasticity in the intrinsic excitability of cortical pyramidal neurons. Nat Neurosci 2:515-520.
DeWire SM, Ahn S, Lefkowitz RJ, Shenoy SK (2007) Beta-arrestins and cell signaling. Annu Rev Physiol 69:483-510.
Ding W, Zhang L, Yan Z, Engelhardt JF (2005) Intracellular trafficking of adeno-associated viral vectors. Gene Ther 12:873-880.
Dolen G, Osterweil E, Rao BS, Smith GB, Auerbach BD, Chattarji S, Bear MF (2007) Correction of fragile X syndrome in mice. Neuron 56:955-962.
Dong JY, Fan PD, Frizzell RA (1996) Quantitative analysis of the packaging capacity of recombinant adeno-associated virus. Hum Gene Ther 7:2101-2112.
Douglas RJ, Martin KA (2004) Neuronal circuits of the neocortex. Annu Rev Neurosci 27:419-451.
Dudek FE, Spitz M (1997) Hypothetical mechanisms for the cellular and neurophysiologic basis of secondary epileptogenesis: proposed role of synaptic reorganization. J Clin Neurophysiol 14:90-101.
Fabene PF et al. (2008) A role for leukocyte-endothelial adhesion mechanisms in epilepsy. Nat Med 14:1377-1383.
Fame RM, MacDonald JL, Macklis JD (2011) Development, specification, and diversity of callosal projection neurons. Trends Neurosci 34:41-50.
Fuentealba P, Crochet S, Steriade M (2004) The cortically evoked secondary depolarization affects the integrative properties of thalamic reticular neurons. Eur J Neurosci 20:2691-2696.
Furtado MA, Castro OW, Del Vecchio F, de Oliveira JA, Garcia-Cairasco N (2011) Study of spontaneous recurrent seizures and morphological alterations after status epilepticus induced by intrahippocampal injection of pilocarpine. Epilepsy Behav 20:257-266.
Goddard GV, McIntyre DC, Leech CK (1969) A permanent change in brain function resulting from daily electrical stimulation. Exp Neurol 25:295-330.
Golarai G, Greenwood AC, Feeney DM, Connor JA (2001) Physiological and structural evidence for hippocampal involvement in persistent seizure susceptibility after traumatic brain injury. J Neurosci 21:8523-8537.
Golshani P, Liu XB, Jones EG (2001) Differences in quantal amplitude reflect GluR4- subunit number at corticothalamic synapses on two populations of thalamic neurons. Proc Natl Acad Sci U S A 98:4172-4177.
Gomes I, Ayoub MA, Fujita W, Jaeger WC, Pfleger KD, Devi LA (2016) G Protein-Coupled Receptor Heteromers. Annu Rev Pharmacol Toxicol 56:403-425.
Gremel CM, Costa RM (2013) Orbitofrontal and striatal circuits dynamically encode the shift between goal-directed and habitual actions. Nat Commun 4:2264.
Grieger JC, Samulski RJ (2005) Adeno-associated virus as a gene therapy vector: vector development, production and clinical applications. Adv Biochem Eng Biotechnol 99:119-145.
Grimm D, Kay MA (2003) From virus evolution to vector revolution: use of naturally occurring serotypes of adeno-associated virus (AAV) as novel vectors for human gene therapy. Curr Gene Ther 3:281-304.
Grone BP, Baraban SC (2015) Animal models in epilepsy research: legacies and new directions. Nat Neurosci 18:339-343.
Gu F, Parada I, Shen F, Li J, Bacci A, Graber K, Taghavi RM, Scalise K, Schwartzkroin P, Wenzel J, Prince DA (2017) Structural alterations in fast-spiking GABAergic interneurons in a model of posttraumatic neocortical epileptogenesis. Neurobiol Dis 108:100-114.
Gupta A, Wang Y, Markram H (2000) Organizing principles for a diversity of GABAergic interneurons and synapses in the neocortex. Science 287:273-278.
Gupta A, Elgammal FS, Proddutur A, Shah S, Santhakumar V (2012) Decrease in tonic inhibition contributes to increase in dentate semilunar granule cell excitability after brain injury. J Neurosci 32:2523-2537.

Haery L, Deverman BE, Matho KS, Cetin A, Woodard K, Cepko C, Guerin KI, Rego MA, Ersing I, Bachle SM, Kamens J, Fan M (2019) Adeno-Associated Virus Technologies and Methods for Targeted Neuronal Manipulation. Front Neuroanat 13:93.

Haggerty DL, Grecco GG, Reeves KC, Atwood B (2020) Adeno-Associated Viral Vectors in Neuroscience Research. Mol Ther Methods Clin Dev 17:69-82.

Harcourt J et al. (2020) Severe Acute Respiratory Syndrome Coronavirus 2 from Patient with Coronavirus Disease, United States. Emerg Infect Dis 26:1266-1273.

Hellier JL, Patrylo PR, Buckmaster PS, Dudek FE (1998) Recurrent spontaneous motor seizures after repeated low-dose systemic treatment with kainate: assessment of a rat model of temporal lobe epilepsy. Epilepsy Res 31:73-84.

Hemingway C, Freeman JM, Pillas DJ, Pyzik PL (2001) The ketogenic diet: a 3- to 6-year follow-up of 150 children enrolled prospectively. Pediatrics 108:898-905.

Herculano-Houzel S (2012) The remarkable, yet not extraordinary, human brain as a scaled-up primate brain and its associated cost. Proc Natl Acad Sci U S A 109 Suppl 1:10661-10668.

Herskovits AZ, Guarente L (2014) SIRT1 in neurodevelopment and brain senescence. Neuron 81:471-483.

Hoffman SN, Salin PA, Prince DA (1994) Chronic neocortical epileptogenesis in vitro. J Neurophysiol 71:1762-1773.

Houser CR, Miyashiro JE, Swartz BE, Walsh GO, Rich JR, Delgado-Escueta AV (1990) Altered patterns of dynorphin immunoreactivity suggest mossy fiber reorganization in human hippocampal epilepsy. J Neurosci 10:267-282.

Houweling AR, Bazhenov M, Timofeev I, Steriade M, Sejnowski TJ (2005) Homeostatic synaptic plasticity can explain post-traumatic epileptogenesis in chronically isolated neocortex. Cereb Cortex 15:834-845.

Hu XL, Cheng X, Cai L, Tan GH, Xu L, Feng XY, Lu TJ, Xiong H, Fei J, Xiong ZQ (2011) Conditional deletion of NRSF in forebrain neurons accelerates epileptogenesis in the kindling model. Cereb Cortex 21:2158-2165.

Huda F, Konno A, Matsuzaki Y, Goenawan H, Miyake K, Shimada T, Hirai H (2014) Distinct transduction profiles in the CNS via three injection routes of AAV9 and the application to generation of a neurodegenerative mouse model. Mol Ther Methods Clin Dev 1:14032.

Hunt RF, Scheff SW, Smith BN (2009) Posttraumatic epilepsy after controlled cortical impact injury in mice. Exp Neurol 215:243-252.

Hunt RF, Scheff SW, Smith BN (2010) Regionally localized recurrent excitation in the dentate gyrus of a cortical contusion model of posttraumatic epilepsy. J Neurophysiol 103:1490-1500.

Hunt RF, Scheff SW, Smith BN (2011) Synaptic reorganization of inhibitory hilar interneuron circuitry after traumatic brain injury in mice. J Neurosci 31:6880-6890.

Hunt RF, Boychuk JA, Smith BN (2013) Neural circuit mechanisms of post-traumatic epilepsy. Front Cell Neurosci 7:89.

Hunt RF, Haselhorst LA, Schoch KM, Bach EC, Rios-Pilier J, Scheff SW, Saatman KE, Smith BN (2012) Posttraumatic mossy fiber sprouting is related to the degree of cortical damage in three mouse strains. Epilepsy Res 99:167-170.

Islam K (2018) The Bump-and-Hole Tactic: Expanding the Scope of Chemical Genetics. Cell Chem Biol 25:1171-1184.

Iyer A, Zurolo E, Prabowo A, Fluiter K, Spliet WG, van Rijen PC, Gorter JA, Aronica E (2012) MicroRNA-146a: a key regulator of astrocyte-mediated inflammatory response. PLoS One 7:e44789.

Jackson KL, Dayton RD, Deverman BE, Klein RL (2016) Better Targeting, Better Efficiency for Wide-Scale Neuronal Transduction with the Synapsin Promoter and AAV-PHP.B. Front Mol Neurosci 9:116.

Jann MW, Lam YW, Chang WH (1994) Rapid formation of clozapine in guinea-pigs and man following clozapine-N-oxide administration. Arch Int Pharmacodyn Ther 328:243-250.

Jendryka M, Palchaudhuri M, Ursu D, van der Veen B, Liss B, Katzel D, Nissen W, Pekcec A (2019) Pharmacokinetic and pharmacodynamic actions of clozapine-N-oxide, clozapine, and compound 21 in DREADD-based chemogenetics in mice. Sci Rep 9:4522.

Jensen MS, Yaari Y (1997) Role of intrinsic burst firing, potassium accumulation, and electrical coupling in the elevated potassium model of hippocampal epilepsy. J Neurophysiol 77:1224-1233.
Jensen MS, Azouz R, Yaari Y (1994) Variant firing patterns in rat hippocampal pyramidal cells modulated by extracellular potassium. J Neurophysiol 71:831-839.
Jin X, Prince DA, Huguenard JR (2006) Enhanced excitatory synaptic connectivity in layer v pyramidal neurons of chronically injured epileptogenic neocortex in rats. J Neurosci 26:4891-4900.
Jin X, Huguenard JR, Prince DA (2011) Reorganization of inhibitory synaptic circuits in rodent chronically injured epileptogenic neocortex. Cereb Cortex 21:1094-1104.
Jong YI, Harmon SK, O'Malley KL (2018) Intracellular GPCRs Play Key Roles in Synaptic Plasticity. ACS Chem Neurosci 9:2162-2172.
Jovicic A, Roshan R, Moisoi N, Pradervand S, Moser R, Pillai B, Luthi-Carter R (2013) Comprehensive expression analyses of neural cell-type-specific miRNAs identify new determinants of the specification and maintenance of neuronal phenotypes. J Neurosci 33:5127-5137.
Jung KH, Chu K, Lee ST, Kim J, Sinn DI, Kim JM, Park DK, Lee JJ, Kim SU, Kim M, Lee SK, Roh JK (2006) Cyclooxygenase-2 inhibitor, celecoxib, inhibits the altered hippocampal neurogenesis with attenuation of spontaneous recurrent seizures following pilocarpine-induced status epilepticus. Neurobiol Dis 23:237-246.
Jyoti A, Sethi P, Sharma D (2009) Curcumin protects against electrobehavioral progression of seizures in the iron-induced experimental model of epileptogenesis. Epilepsy Behav 14:300-308.
Kaas JH (2013) The evolution of brains from early mammals to humans. Wiley Interdiscip Rev Cogn Sci 4:33-45.
Kadam SD, White AM, Staley KJ, Dudek FE (2010) Continuous electroencephalographic monitoring with radio-telemetry in a rat model of perinatal hypoxia-ischemia reveals progressive post-stroke epilepsy. J Neurosci 30:404-415.
Kandratavicius L, Balista PA, Lopes-Aguiar C, Ruggiero RN, Umeoka EH, Garcia-Cairasco N, Bueno-Junior LS, Leite JP (2014) Animal models of epilepsy: use and limitations. Neuropsychiatr Dis Treat 10:1693-1705.
Kawaguchi Y, Kubota Y (1997) GABAergic cell subtypes and their synaptic connections in rat frontal cortex. Cereb Cortex 7:476-486.
Kilman V, van Rossum MC, Turrigiano GG (2002) Activity deprivation reduces miniature IPSC amplitude by decreasing the number of postsynaptic GABA(A) receptors clustered at neocortical synapses. J Neurosci 22:1328-1337.
Kita T, Kita H (2012) The subthalamic nucleus is one of multiple innervation sites for long-range corticofugal axons: a single-axon tracing study in the rat. J Neurosci 32:5990-5999.
Kobow K, Kaspi A, Harikrishnan KN, Kiese K, Ziemann M, Khurana I, Fritzsche I, Hauke J, Hahnen E, Coras R, Muhlebner A, El-Osta A, Blumcke I (2013) Deep sequencing reveals increased DNA methylation in chronic rat epilepsy. Acta Neuropathol 126:741-756.
Kochanek PM, Vagni VA, Janesko KL, Washington CB, Crumrine PK, Garman RH, Jenkins LW, Clark RS, Homanics GE, Dixon CE, Schnermann J, Jackson EK (2006) Adenosine A1 receptor knockout mice develop lethal status epilepticus after experimental traumatic brain injury. J Cereb Blood Flow Metab 26:565-575.
Kojima N, Borlikova G, Sakamoto T, Yamada K, Ikeda T, Itohara S, Niki H, Endo S (2008) Inducible cAMP early repressor acts as a negative regulator for kindling epileptogenesis and long-term fear memory. J Neurosci 28:6459-6472.
Krashes MJ, Koda S, Ye C, Rogan SC, Adams AC, Cusher DS, Maratos-Flier E, Roth BL, Lowell BB (2011) Rapid, reversible activation of AgRP neurons drives feeding behavior in mice. J Clin Invest 121:1424-1428.
Kugler S, Kilic E, Bahr M (2003) Human synapsin 1 gene promoter confers highly neuron-specific long-term transgene expression from an adenoviral vector in the adult rat brain depending on the transduced area. Gene Ther 10:337-347.

Kusmierczak M, Lajeunesse F, Grand L, Timofeev I (2015) Changes in long-range connectivity and neuronal reorganization in partial cortical deafferentation model of epileptogenesis. Neuroscience 284:153-164.
Landisman CE, Long MA, Beierlein M, Deans MR, Paul DL, Connors BW (2002) Electrical synapses in the thalamic reticular nucleus. J Neurosci 22:1002-1009.
Lanza AM, Dyess TJ, Alper HS (2012) Using the Cre/lox system for targeted integration into the human genome: loxFAS-loxP pairing and delayed introduction of Cre DNA improve gene swapping efficiency. Biotechnol J 7:898-908.
Lemieux M, Chen JY, Lonjers P, Bazhenov M, Timofeev I (2014) The impact of cortical deafferentation on the neocortical slow oscillation. J Neurosci 34:5689-5703.
Lentz TB, Gray SJ, Samulski RJ (2012) Viral vectors for gene delivery to the central nervous system. Neurobiol Dis 48:179-188.
Lerch TF, O'Donnell JK, Meyer NL, Xie Q, Taylor KA, Stagg SM, Chapman MS (2012) Structure of AAV-DJ, a retargeted gene therapy vector: cryo-electron microscopy at 4.5 A resolution. Structure 20:1310-1320.
Letinic K, Zoncu R, Rakic P (2002) Origin of GABAergic neurons in the human neocortex. Nature 417:645-649.
Li H, Prince DA (2002) Synaptic activity in chronically injured, epileptogenic sensory-motor neocortex. J Neurophysiol 88:2-12.
Li H, McDonald W, Parada I, Faria L, Graber K, Takahashi DK, Ma Y, Prince D (2011) Targets for preventing epilepsy following cortical injury. Neurosci Lett 497:172-176.
Liao D, Scannevin RH, Huganir R (2001) Activation of silent synapses by rapid activity-dependent synaptic recruitment of AMPA receptors. J Neurosci 21:6008-6017.
Lieb A, Weston M, Kullmann DM (2019) Designer receptor technology for the treatment of epilepsy. EBioMedicine 43:641-649.
Lissin DV, Gomperts SN, Carroll RC, Christine CW, Kalman D, Kitamura M, Hardy S, Nicoll RA, Malenka RC, von Zastrow M (1998) Activity differentially regulates the surface expression of synaptic AMPA and NMDA glutamate receptors. Proc Natl Acad Sci U S A 95:7097-7102.
Lizee G, Aerts JL, Gonzales MI, Chinnasamy N, Morgan RA, Topalian SL (2003) Real-time quantitative reverse transcriptase-polymerase chain reaction as a method for determining lentiviral vector titers and measuring transgene expression. Hum Gene Ther 14:497-507.
Loscher W (1997) Animal models of intractable epilepsy. Prog Neurobiol 53:239-258.
Loscher W (2017) Animal Models of Seizures and Epilepsy: Past, Present, and Future Role for the Discovery of Antiseizure Drugs. Neurochem Res 42:1873-1888.
Lothman EW, Bertram EH, 3rd, Stringer JL (1991) Functional anatomy of hippocampal seizures. Prog Neurobiol 37:1-82.
Luppi PH, Clement O, Fort P (2013) Paradoxical (REM) sleep genesis by the brainstem is under hypothalamic control. Curr Opin Neurobiol 23:786-792.
Lynch M, Sutula T (2000) Recurrent excitatory connectivity in the dentate gyrus of kindled and kainic acid-treated rats. J Neurophysiol 83:693-704.
Manvich DF, Webster KA, Foster SL, Farrell MS, Ritchie JC, Porter JH, Weinshenker D (2018) The DREADD agonist clozapine N-oxide (CNO) is reverse-metabolized to clozapine and produces clozapine-like interoceptive stimulus effects in rats and mice. Sci Rep 8:3840.
Markram H, Toledo-Rodriguez M, Wang Y, Gupta A, Silberberg G, Wu C (2004) Interneurons of the neocortical inhibitory system. Nat Rev Neurosci 5:793-807.
Marsh EB, Freeman JM, Kossoff EH, Vining EP, Rubenstein JE, Pyzik PL, Hemingway C (2006) The outcome of children with intractable seizures: a 3- to 6-year follow-up of 67 children who remained on the ketogenic diet less than one year. Epilepsia 47:425-430.
McClelland S, Brennan GP, Dube C, Rajpara S, Iyer S, Richichi C, Bernard C, Baram TZ (2014) The transcription factor NRSF contributes to epileptogenesis by selective repression of a subset of target genes. Elife 3:e01267.
McCormick DA, Contreras D (2001) On the cellular and network bases of epileptic seizures. Annu Rev Physiol 63:815-846.

McDaniel SS, Wong M (2011) Therapeutic role of mammalian target of rapamycin (mTOR) inhibition in preventing epileptogenesis. Neurosci Lett 497:231-239.
Mountcastle VB (1957) Modality and topographic properties of single neurons of cat's somatic sensory cortex. J Neurophysiol 20:408-434.
Mountcastle VB (1997) The columnar organization of the neocortex. Brain 120 (Pt 4):701-722.
Mtchedlishvili Z, Lepsveridze E, Xu H, Kharlamov EA, Lu B, Kelly KM (2010) Increase of GABAA receptor-mediated tonic inhibition in dentate granule cells after traumatic brain injury. Neurobiol Dis 38:464-475.
Murthy VN, Schikorski T, Stevens CF, Zhu Y (2001) Inactivity produces increases in neurotransmitter release and synapse size. Neuron 32:673-682.
Nadler JV, Perry BW, Cotman CW (1980) Selective reinnervation of hippocampal area CA1 and the fascia dentata after destruction of CA3-CA4 afferents with kainic acid. Brain Res 182:1-9.
Nagai Y et al. (2020) Deschloroclozapine, a potent and selective chemogenetic actuator enables rapid neuronal and behavioral modulations in mice and monkeys. Nat Neurosci 23:1157-1167.
Neal EG, Chaffe H, Schwartz RH, Lawson MS, Edwards N, Fitzsimmons G, Whitney A, Cross JH (2008) The ketogenic diet for the treatment of childhood epilepsy: a randomised controlled trial. Lancet Neurol 7:500-506.
Nilsson P, Ronne-Engstrom E, Flink R, Ungerstedt U, Carlson H, Hillered L (1994) Epileptic seizure activity in the acute phase following cortical impact trauma in rat. Brain Res 637:227-232.
Nissinen J, Halonen T, Koivisto E, Pitkanen A (2000) A new model of chronic temporal lobe epilepsy induced by electrical stimulation of the amygdala in rat. Epilepsy Res 38:177-205.
Nita DA, Cisse Y, Timofeev I, Steriade M (2007) Waking-sleep modulation of paroxysmal activities induced by partial cortical deafferentation. Cereb Cortex 17:272-283.
O'Brien RJ, Kamboj S, Ehlers MD, Rosen KR, Fischbach GD, Huganir RL (1998) Activity-dependent modulation of synaptic AMPA receptor accumulation. Neuron 21:1067-1078.
Patel A, Pyzik PL, Turner Z, Rubenstein JE, Kossoff EH (2010) Long-term outcomes of children treated with the ketogenic diet in the past. Epilepsia 51:1277-1282.
Patrylo PR, Dudek FE (1998) Physiological unmasking of new glutamatergic pathways in the dentate gyrus of hippocampal slices from kainate-induced epileptic rats. J Neurophysiol 79:418-429.
Pavlov I, Huusko N, Drexel M, Kirchmair E, Sperk G, Pitkanen A, Walker MC (2011) Progressive loss of phasic, but not tonic, GABAA receptor-mediated inhibition in dentate granule cells in a model of post-traumatic epilepsy in rats. Neuroscience 194:208-219.
Peters A, Sethares C (1991) Organization of pyramidal neurons in area 17 of monkey visual cortex. J Comp Neurol 306:1-23.
Pinault D, Leresche N, Charpier S, Deniau JM, Marescaux C, Vergnes M, Crunelli V (1998) Intracellular recordings in thalamic neurones during spontaneous spike and wave discharges in rats with absence epilepsy. J Physiol 509 (Pt 2):449-456.
Ping X, Jin X (2016) Chronic Posttraumatic Epilepsy following Neocortical Undercut Lesion in Mice. PLoS One 11:e0158231.
Pitkanen A, Lukasiuk K, Dudek FE, Staley KJ (2015) Epileptogenesis. Cold Spring Harb Perspect Med 5.
Porter BE, Lund IV, Varodayan FP, Wallace RW, Blendy JA (2008) The role of transcription factors cyclic-AMP responsive element modulator (CREM) and inducible cyclic-AMP early repressor (ICER) in epileptogenesis. Neuroscience 152:829-836.
Porter LL, White EL (1986) Synaptic connections of callosal projection neurons in the vibrissal region of mouse primary motor cortex: an electron microscopic/horseradish peroxidase study. J Comp Neurol 248:573-587.
Prince DA, Tseng GF (1993) Epileptogenesis in chronically injured cortex: in vitro studies. J Neurophysiol 69:1276-1291.
Prince DA, Parada I, Graber K (2012) Traumatic Brain Injury and Posttraumatic Epilepsy. In: Jasper's Basic Mechanisms of the Epilepsies (th, Noebels JL, Avoli M, Rogawski MA, Olsen RW, Delgado-Escueta AV, eds). Bethesda (MD).
Qiu J, Pintel D (2008) Processing of adeno-associated virus RNA. Front Biosci 13:3101-3115.

Qiu LF, Lu TJ, Hu XL, Yi YH, Liao WP, Xiong ZQ (2009) Limbic epileptogenesis in a mouse model of fragile X syndrome. Cereb Cortex 19:1504-1514.
Raible DJ, Frey LC, Cruz Del Angel Y, Russek SJ, Brooks-Kayal AR (2012) GABA(A) receptor regulation after experimental traumatic brain injury. J Neurotrauma 29:2548-2554.
Ramaswamy S, Markram H (2015) Anatomy and physiology of the thick-tufted layer 5 pyramidal neuron. Front Cell Neurosci 9:233.
Rao A, Craig AM (1997) Activity regulates the synaptic localization of the NMDA receptor in hippocampal neurons. Neuron 19:801-812.
Ravizza T, Balosso S, Vezzani A (2011) Inflammation and prevention of epileptogenesis. Neurosci Lett 497:223-230.
Ren JQ, Aika Y, Heizmann CW, Kosaka T (1992) Quantitative analysis of neurons and glial cells in the rat somatosensory cortex, with special reference to GABAergic neurons and parvalbumin-containing neurons. Exp Brain Res 92:1-14.
Ribeiro-Oliveira R, Vojtek M, Goncalves-Monteiro S, Vieira-Rocha MS, Sousa JB, Goncalves J, Diniz C (2019) Nuclear G-protein-coupled receptors as putative novel pharmacological targets. Drug Discov Today 24:2192-2201.
Roth BL (2016) DREADDs for Neuroscientists. Neuron 89:683-694.
Rougeul A, Letalle A, Corvisier J (1972) [Rhythmic activity of the primary somatosensory cortex in relation to immobility in the unrestrained awake cat]. Electroencephalogr Clin Neurophysiol 33:23-39.
Rougeul-Buser A, Bouyer JJ, Buser P (1975) From attentiveness to sleep. A topographical analysis of localized "synchronized" activities on the cortex of normal cat and monkey. Acta Neurobiol Exp (Wars) 35:805-819.
Rowe RK, Griffiths DR, Lifshitz J (2016) Midline (Central) Fluid Percussion Model of Traumatic Brain Injury. Methods Mol Biol 1462:211-230.
Ruffolo RR, Jr. (1982) Review important concepts of receptor theory. J Auton Pharmacol 2:277-295.
Rutherford LC, Nelson SB, Turrigiano GG (1998) BDNF has opposite effects on the quantal amplitude of pyramidal neuron and interneuron excitatory synapses. Neuron 21:521-530.
Rutherford LC, DeWan A, Lauer HM, Turrigiano GG (1997) Brain-derived neurotrophic factor mediates the activity-dependent regulation of inhibition in neocortical cultures. J Neurosci 17:4527-4535.
Salegio EA, Samaranch L, Kells AP, Mittermeyer G, San Sebastian W, Zhou S, Beyer J, Forsayeth J, Bankiewicz KS (2013) Axonal transport of adeno-associated viral vectors is serotype-dependent. Gene Ther 20:348-352.
Salin P, Tseng GF, Hoffman S, Parada I, Prince DA (1995) Axonal sprouting in layer V pyramidal neurons of chronically injured cerebral cortex. J Neurosci 15:8234-8245.
Scharfman HE (2005) Brain-derived neurotrophic factor and epilepsy--a missing link? Epilepsy Curr 5:83-88.
Shabram P, Aguilar-Cordova E (2000) Multiplicity of infection/multiplicity of confusion. Mol Ther 2:420-421.
Shao LR, Dudek FE (2005) Changes in mIPSCs and sIPSCs after kainate treatment: evidence for loss of inhibitory input to dentate granule cells and possible compensatory responses. J Neurophysiol 94:952-960.
Sharma AK, Reams RY, Jordan WH, Miller MA, Thacker HL, Snyder PW (2007) Mesial temporal lobe epilepsy: pathogenesis, induced rodent models and lesions. Toxicol Pathol 35:984-999.
Shchepinova MM, Hanyaloglu AC, Frost GS, Tate EW (2020) Chemical biology of noncanonical G protein-coupled receptor signaling: Toward advanced therapeutics. Curr Opin Chem Biol 56:98-110.
Shibley H, Smith BN (2002) Pilocarpine-induced status epilepticus results in mossy fiber sprouting and spontaneous seizures in C57BL/6 and CD-1 mice. Epilepsy Res 49:109-120.
Smith GJ, Dunkley WL (1962) Initiation of lipid peroxidation by a reduced metal ion. Arch Biochem Biophys 98:46-48.
Smith JS, Lefkowitz RJ, Rajagopal S (2018) Biased signalling: from simple switches to allosteric microprocessors. Nat Rev Drug Discov 17:243-260.
Smith KS, Bucci DJ, Luikart BW, Mahler SV (2016) DREADDS: Use and application in behavioral neuroscience. Behav Neurosci 130:137-155.

Somogyi P, Tamas G, Lujan R, Buhl EH (1998) Salient features of synaptic organisation in the cerebral cortex. Brain Res Brain Res Rev 26:113-135.
Sonntag F, Kother K, Schmidt K, Weghofer M, Raupp C, Nieto K, Kuck A, Gerlach B, Bottcher B, Muller OJ, Lux K, Horer M, Kleinschmidt JA (2011) The assembly-activating protein promotes capsid assembly of different adeno-associated virus serotypes. J Virol 85:12686-12697.
Sposini S, Jean-Alphonse FG, Ayoub MA, Oqua A, West C, Lavery S, Brosens JJ, Reiter E, Hanyaloglu AC (2017) Integration of GPCR Signaling and Sorting from Very Early Endosomes via Opposing APPL1 Mechanisms. Cell Rep 21:2855-2867.
Srivastava S (2016) Emerging therapeutic roles for NAD(+) metabolism in mitochondrial and age-related disorders. Clin Transl Med 5:25.
Stachniak TJ, Ghosh A, Sternson SM (2014) Chemogenetic synaptic silencing of neural circuits localizes a hypothalamus-->midbrain pathway for feeding behavior. Neuron 82:797-808.
Staiger JF, Flagmeyer I, Schubert D, Zilles K, Kotter R, Luhmann HJ (2004) Functional diversity of layer IV spiny neurons in rat somatosensory cortex: quantitative morphology of electrophysiologically characterized and biocytin labeled cells. Cereb Cortex 14:690-701.
Stellwagen D, Beattie EC, Seo JY, Malenka RC (2005) Differential regulation of AMPA receptor and GABA receptor trafficking by tumor necrosis factor-alpha. J Neurosci 25:3219-3228.
Steriade M (2006) Grouping of brain rhythms in corticothalamic systems. Neuroscience 137:1087-1106.
Steriade M, Contreras D (1998) Spike-wave complexes and fast components of cortically generated seizures. I. Role of neocortex and thalamus. J Neurophysiol 80:1439-1455.
Steriade M, Timofeev I, Grenier F (2001) Natural waking and sleep states: a view from inside neocortical neurons. J Neurophysiol 85:1969-1985.
Sternson SM, Roth BL (2014) Chemogenetic tools to interrogate brain functions. Annu Rev Neurosci 37:387-407.
Sutula T, Cascino G, Cavazos J, Parada I, Ramirez L (1989) Mossy fiber synaptic reorganization in the epileptic human temporal lobe. Ann Neurol 26:321-330.
Sutula TP (2004) Mechanisms of epilepsy progression: current theories and perspectives from neuroplasticity in adulthood and development. Epilepsy Res 60:161-171.
Sutula TP, Dudek FE (2007) Unmasking recurrent excitation generated by mossy fiber sprouting in the epileptic dentate gyrus: an emergent property of a complex system. Prog Brain Res 163:541-563.
Tan L, Yan W, McCorvy JD, Cheng J (2018) Biased Ligands of G Protein-Coupled Receptors (GPCRs): Structure-Functional Selectivity Relationships (SFSRs) and Therapeutic Potential. J Med Chem 61:9841-9878.
Tauck DL, Nadler JV (1985) Evidence of functional mossy fiber sprouting in hippocampal formation of kainic acid-treated rats. J Neurosci 5:1016-1022.
Tehrani MH, Barnes EM, Jr. (1988) GABA down-regulates the GABA/benzodiazepine receptor complex in developing cerebral neurons. Neurosci Lett 87:288-292.
Thio LL, Erbayat-Altay E, Rensing N, Yamada KA (2006) Leptin contributes to slower weight gain in juvenile rodents on a ketogenic diet. Pediatr Res 60:413-417.
Thompson KJ et al. (2018) DREADD Agonist 21 Is an Effective Agonist for Muscarinic-Based DREADDs in Vitro and in Vivo. ACS Pharmacol Transl Sci 1:61-72.
Thomsen ARB, Jensen DD, Hicks GA, Bunnett NW (2018) Therapeutic Targeting of Endosomal G-Protein-Coupled Receptors. Trends Pharmacol Sci 39:879-891.
Thomson AM (2010) Neocortical layer 6, a review. Front Neuroanat 4:13.
Timofeev I (2011) Injury induced epileptogenesis: contribution of active inhibition, disfacilitation and deafferentation to seizure induction in thalamocortical system. In: Inhibitory Synaptic Plasticity (Woodin MA, Maffei A, eds). New York: Springer.
Timofeev I, Steriade M (2004) Neocortical seizures: initiation, development and cessation. Neuroscience 123:299-336.
Timofeev I, Bazhenov M (2005) Mechanisms of cortical trauma induced epileptogenesis and seizures. In: Recent Res. Devel. Physiol. Kerala, India: Pandalai, SG, ed.).

Timofeev I, Chauvette S (2013) The spindles: are they still thalamic? Sleep 36:825-826.
Timofeev I, Grenier F, Steriade M (1998) Spike-wave complexes and fast components of cortically generated seizures. IV. Paroxysmal fast runs in cortical and thalamic neurons. J Neurophysiol 80:1495-1513.
Timofeev I, Grenier F, Steriade M (2001) Disfacilitation and active inhibition in the neocortex during the natural sleep-wake cycle: an intracellular study. Proc Natl Acad Sci U S A 98:1924-1929.
Timofeev I, Grenier F, Steriade M (2002) The role of chloride-dependent inhibition and the activity of fast-spiking neurons during cortical spike-wave electrographic seizures. Neuroscience 114:1115-1132.
Timofeev I, Chauvette S, Soltani S (2014) Neocortical focus: experimental view. Int Rev Neurobiol 114:9-33.
Timofeev I, Bazhenov M, Avramescu S, Nita DA (2010) Posttraumatic epilepsy: the roles of synaptic plasticity. Neuroscientist 16:19-27.
Timofeev I, Sejnowski TJ, Bazhenov M, Chauvette S, Grand LB (2013) Age dependency of trauma-induced neocortical epileptogenesis. Front Cell Neurosci 7:154.
Timofeev IB, M. (2005) Mechanisms of cortical trauma-induced epileptogenesis and seizures. In: Recent Res. Devel. Physiol. (Pandalai, SG, ed.). India: Kerala.
Topolnik L, Steriade M, Timofeev I (2003a) Hyperexcitability of intact neurons underlies acute development of trauma-related electrographic seizures in cats in vivo. Eur J Neurosci 18:486-496.
Topolnik L, Steriade M, Timofeev I (2003b) Partial cortical deafferentation promotes development of paroxysmal activity. Cereb Cortex 13:883-893.
Traub RD, Wong RK (1982) Cellular mechanism of neuronal synchronization in epilepsy. Science 216:745-747.
Turrigiano GG (1999) Homeostatic plasticity in neuronal networks: the more things change, the more they stay the same. Trends Neurosci 22:221-227.
Turrigiano GG, Nelson SB (1998) Thinking globally, acting locally: AMPA receptor turnover and synaptic strength. Neuron 21:933-935.
Van Horn SC, Sherman SM (2007) Fewer driver synapses in higher order than in first order thalamic relays. Neuroscience 146:463-470.
Vardy E et al. (2015) A New DREADD Facilitates the Multiplexed Chemogenetic Interrogation of Behavior. Neuron 86:936-946.
Vazey EM, Aston-Jones G (2014) Designer receptor manipulations reveal a role of the locus coeruleus noradrenergic system in isoflurane general anesthesia. Proc Natl Acad Sci U S A 111:3859-3864.
Veinante P, Deschenes M (2003) Single-cell study of motor cortex projections to the barrel field in rats. J Comp Neurol 464:98-103.
Vergnes M, Marescaux C, Micheletti G, Reis J, Depaulis A, Rumbach L, Warter JM (1982) Spontaneous paroxysmal electroclinical patterns in rat: a model of generalized non-convulsive epilepsy. Neurosci Lett 33:97-101.
Wang Q, Zhou FM (2019) cAMP-producing chemogenetic and adenosine A2a receptor activation inhibits the inwardly rectifying potassium current in striatal projection neurons. Neuropharmacology 148:229-243.
Wang SJ, Zhao XH, Chen W, Bo N, Wang XJ, Chi ZF, Wu W (2015) Sirtuin 1 activation enhances the PGC-1alpha/mitochondrial antioxidant system pathway in status epilepticus. Mol Med Rep 11:521-526.
Wang Y, Menon N, Shen S, Feschenko M, Bergelson S (2020) A qPCR Method for AAV Genome Titer with ddPCR-Level of Accuracy and Precision. Mol Ther Methods Clin Dev 19:341-346.
Wang Y, Chen Y, Xu W, Lee DY, Ma Z, Rawls SM, Cowan A, Liu-Chen LY (2008) 2-Methoxymethyl-salvinorin B is a potent kappa opioid receptor agonist with longer lasting action in vivo than salvinorin A. J Pharmacol Exp Ther 324:1073-1083.
Watt AJ, van Rossum MC, MacLeod KM, Nelson SB, Turrigiano GG (2000) Activity coregulates quantal AMPA and NMDA currents at neocortical synapses. Neuron 26:659-670.
Weis WI, Kobilka BK (2018) The Molecular Basis of G Protein-Coupled Receptor Activation. Annu Rev Biochem 87:897-919.
Williams PA, White AM, Clark S, Ferraro DJ, Swiercz W, Staley KJ, Dudek FE (2009) Development of spontaneous recurrent seizures after kainate-induced status epilepticus. J Neurosci 29:2103-2112.
Willmore LJ (2012) Posttraumatic Epilepsy: What's Contusion Got to Do With It? Epilepsy Curr 12:87-91.

Willmore LJ, Rubin JJ (1981) Antiperoxidant pretreatment and iron-induced epileptiform discharges in the rat: EEG and histopathologic studies. Neurology 31:63-69.
Willmore LJ, Rubin JJ (1984) Effects of antiperoxidants on FeCl2-induced lipid peroxidation and focal edema in rat brain. Exp Neurol 83:62-70.
Willmore LJ, Ueda Y (2009) Posttraumatic epilepsy: hemorrhage, free radicals and the molecular regulation of glutamate. Neurochem Res 34:688-697.
Winokur RS, Kubal T, Liu D, Davis SF, Smith BN (2004) Recurrent excitation in the dentate gyrus of a murine model of temporal lobe epilepsy. Epilepsy Res 58:93-105.
Wuarin JP, Dudek FE (1996) Electrographic seizures and new recurrent excitatory circuits in the dentate gyrus of hippocampal slices from kainate-treated epileptic rats. J Neurosci 16:4438-4448.
Wuarin JP, Dudek FE (2001) Excitatory synaptic input to granule cells increases with time after kainate treatment. J Neurophysiol 85:1067-1077.
Yasi EA, Kruyer NS, Peralta-Yahya P (2020) Advances in G protein-coupled receptor high-throughput screening. Curr Opin Biotechnol 64:210-217.
Zeng LH, McDaniel S, Rensing NR, Wong M (2010) Regulation of cell death and epileptogenesis by the mammalian target of rapamycin (mTOR): a double-edged sword? Cell Cycle 9:2281-2285.
Zhang N, Houser CR (1999) Ultrastructural localization of dynorphin in the dentate gyrus in human temporal lobe epilepsy: a study of reorganized mossy fiber synapses. J Comp Neurol 405:472-490.
Zhang W, Yamawaki R, Wen X, Uhl J, Diaz J, Prince DA, Buckmaster PS (2009) Surviving hilar somatostatin interneurons enlarge, sprout axons, and form new synapses with granule cells in a mouse model of temporal lobe epilepsy. J Neurosci 29:14247-14256.
Zhou QG, Nemes AD, Lee D, Ro EJ, Zhang J, Nowacki AS, Dymecki SM, Najm IM, Suh H (2019) Chemogenetic silencing of hippocampal neurons suppresses epileptic neural circuits. J Clin Invest 129:310-323.
Zingg B, Chou XL, Zhang ZG, Mesik L, Liang F, Tao HW, Zhang LI (2017) AAV-Mediated Anterograde Transsynaptic Tagging: Mapping Corticocollicular Input-Defined Neural Pathways for Defense Behaviors. Neuron 93:33-47.